Oil and Gas Field Application of Hydrate Kinetics Modeling

by Trevor Roberts

A Thesis submitted

to the School of Graduate Studies in partial fulfillment of the

requirements for the degree of

Master of Engineering (MEng)

Faculty of Engineering and Applied Science

Memorial University of Newfoundland

May 2019

St. John’s Newfoundland and Labrador

ABSTRACT

In the offshore environments, hydrocarbons are extracted from the reservoir and transported through subsea flowlines in which ambient temperatures can be as low as 0°C. The production systems must be designed to manage potential gas hydrate formation which can lead to pipe blockages.

This thesis assessed the applicability of coupling multiphase Oil and Gas Simulator (OLGA) models with a hydrate prediction model (Colorado School of Mines Hydrate Kinetics) as a tool to better understand the risk with hydrate blockages. This tool would be more realistic than the current method of using hydrate dissociation curves, which can tend to be conservative.

Real oil field data is used to validate the coupled model results. Two example cases were analyzed in this work, 1) hydrate blockage had formed and 2) conditions present for hydrate risk. In the first case it was found that the sub cooling (the difference between the flowline and hydrate formation temperatures) assumption may have been conservative, and the model did correctly predict the most likely location of the blockage based on vol% of formed hydrate. In the second case the model confirmed that there was little hydrate formed and in reality there were no signs of blockages upon restart of the flowlines.

Overall the analyses showed that the coupled model can be a useful tool for hydrate prediction. Modifications were proposed to improve the modelling predictions by incorporating the impact of the sub cooling and its stochastic nature within the model. Another potential improvement could be integrating compositional tracking in the model to constantly generate hydrate curves in each volume section of the models based on the expected fluid content. It is also proposed to further the understanding of water/oil emulsion in the kinetics of hydrate and hydrate plug formation.

Table of Contents

LIST OF TABLES

LIST OF FIGURES

1.0 Introduction

1.1 Overview of an offshore oil and gas development

Hydrocarbons can exist in the forms of a solid (coal), liquid (oil or condensate), or a gas and are the result of decomposition of organic matter over millions of years within the earth. Hydrocarbons are generally located deep in geological traps within the pores of the formation rock. To have a hydrocarbon reservoir the following criteria must be met; a cap rock or seal must exist above the reservoir layer; the reservoir layer must have good porosity/permeability, so fluids can flow, and this must finally line up over geological time in order to have the hydrocarbons migrate into the reservoir.

In the offshore oil and gas industry the hydrocarbon reservoir is classified as a conventional resource. That is the fluids can be exploited to flow naturally by means of drilling a traditional well into the formation. To exploit offshore hydrocarbon resources, wells are drilled deep into the earth where they intersect the fluid bearing reservoirs. To economically sustain an offshore development these reservoirs should be prolific in fluid production when compared to an onshore development. In simple terms a hydrocarbon reservoir can be thought of a pressurized tank of fluids. To exploit these resources, wells are placed within the tank where the fluids can flow back to surface. Water or gas injection wells are also utilized to sustain the pressures within the tank and sweep the hydrocarbons. Over time it may be inevitable that pressure falls or the reservoir water flow to wells increase and therefore methods of artificial lift may be required. One of the most common methods of artificial lift is the use of gas to lift the liquids in the well. In this method associated gas is injected down the annulus of a production well into the production tubing to lighten the fluid column.

In order to produce these wells, they are connected back to a production and process facility which for offshore developments could be a Floating Production Storage and Offloading (FPSO) facility or some sort of host platform above the water. These connections include various flowlines which are laid on the seabed and connected through risers. It is important to ensure the design and operations of the infrastructure are properly completed over the field's expected life conditions (pressures, temperatures, and fluid compositions). This work falls into the discipline of Flow Assurance, which will be discussed in the next section.

1.2 Overview of Flow Assurance

Flow Assurance in the simplest terms can be described as the guarantee of flow of fluids. High costs of intervention/equipment and prolificacy of offshore oil and gas wells mean any interrupted flow it can have significant economic losses; hence the importance of the Flow Assurance.

Flow Assurance includes areas of science and engineering that deal with flow of fluids within the production systems. In Flow Assurance, the operation of an oil and gas system is studied holistically from start-up, steady state, shutdown, and any other expected operating scenarios of the fluid handling infrastructure. Common issues typically dealt with in Flow Assurance include: hydrates, high or low temperature effects e.g., Joule Thomson (JT) effect, wax deposition, scaling, potential for formation of asphaltenes, and impact of fluid velocity in

corrosion and erosion of the production systems. Throughout the life of an oil and gas field the pressures, temperatures, and composition of fluids can vary greatly. Thus, dealing with Flow Assurance issues must be well thought out and the systems designed to operate safely and efficiently.

In designing an offshore subsea oil and gas production system one of the main challenges is to avoid hydrate formation during operation. An oil and gas development will always deal with multiphase fluids (oil, gas, and aqueous phases). These fluids are produced from naturally pressurized reservoirs that are connected to the surface through wells. In the case of offshore developments, the wells are connected via pipework and flowlines that eventually end up at a processing platform. In many subsea developments the seafloor temperatures are close to 0 °C; this creates ideal environments for pressurized hydrocarbon gas and water to generate hydrates which are snow/ice like substances. Deeper water depths also magnify higher operating pressures within production flowlines, since the natural head in risers magnifies operating pressures.

Hydrates can create blockages within equipment which can be safety hazards by forming blockages (ice/snow like plugs). Under the right conditions they can be become hazardous projectiles, thus understanding potential locations of any type of blockage is important. Remediation efforts can take an extensive amount of time depending on the severity of the blockage and options available to dissociate. A common task that is carried out within flow assurance area is prescribing a “no touch time” (NTT) for a field, which is defined as the time fluids can be left stagnant in the production flowlines before hydrate could form and the system could safely be restarted. The time it takes for the flowlines temperature reaches the temperature where the hydrate could form, at the operating pressure of the flowlines, is called “cool down” period. The numerical difference between the hydrate formation temperature and the actual fluids temperature in the flowline is called “sub cooling”. If a system is left stagnant longer than the cool down period and beyond its NTT it generally must be depressurized (to dissociate hydrate) or hot fluids must be circulated, which can be time consuming.

1.3 Objective of Study

The objective of this study is to assess coupling the Colorado School of Mines Hydrate Kinetics (CSMHyK) model with the dynamic multiphase simulator OLGA for use as a practical engineering tool in predicting hydrate formation and flowline plugging potential for design and troubleshooting purposes.

To illustrate this, actual oil field data was used to support the analyses performed in the following cases:

Case 1: A hydrate blockage had formed within an untreated production spool.

Case 2: Conditions was present within a complex subsea flowline system for hydrate to form according to field operating guidelines.

2.0 Hydrates and modeling tools

2.1 Overview of Hydrates and Design

A hydrate is a solid substance that forms when a gas comes into contact with water at the correct temperature and pressure. Gas hydrates are classified as a clathrate compound because on a molecular level a lattice structure is formed from gas molecules that house the water molecules. The three common hydrate are generally known as SI, SII, and SH [1]. Figure 1 outlines the form of these structures [1].

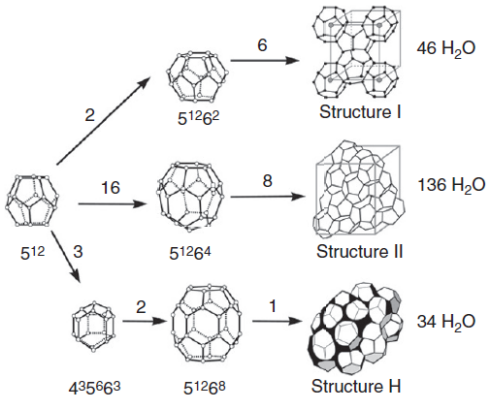

Figure 1.1 The three repeating hydrate unit crystals and their constitutive cages.

Figure 1: Illustration of SI, SII, and SH hydrate structures **[1]**

The water molecules bond together to create cages around the guest gas molecule. Depending on the size of the gas molecules it will determine what hydrate structure it can form. The oil and gas industries predominantly face challenges with SII hydrate structures [1]. The guest gas molecules that generally fill these voids include methane, ethane, propane, and butane [1]. The pressure, temperature, and fluid composition will dictate the hydrate physical properties such as density and hardness. A hydrates physical appearance and how it agglomerates can be compared to snow and ice. Figure 2 illustrates a hydrate that appears fluffy, has porosity, and is less dense while Figure 3 shows a very solid looking hydrate plug likely with little porosity and much denser.

Within the oil and gas industry, hydrate formation was first identified in onshore gas flowlines where temperatures was above 0°C [2] .The major concern for oil and gas installations is the risk of plugging equipment by hydrate formation, which can pose as a safety hazard and cause operational inefficiencies.

Figure 2: Hydrate Physical Characteristics **[3]**

Figure 3: Hard Hydrate Physical Characteristics **[4]**

When designing oil and gas facilities, hydrate dissociation curves are generated using thermodynamic packages based on the expected gas composition. The hydrate dissociation curves represent the pressures and temperatures at which hydrate crystals can exist. Figure 4 illustrates an example of a hydrate dissociation curve.

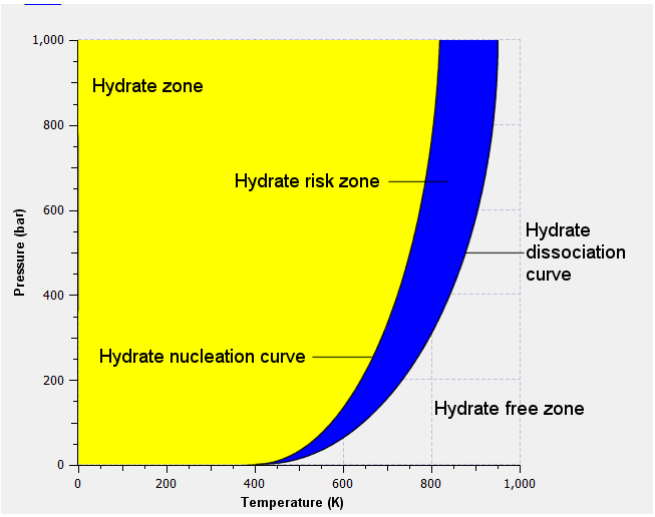

Figure 4: Hydrate dissociation and nucleation curve **[5]**

Anywhere to the left of the hydrate dissociation curve represents temperature and pressures where a hydrate has the potential to form and be thermodynamically stable. Time and sub-

cooling is initially required to form a hydrate crystal; sub-cooling represents how far the temperature is from the dissociation temperature for a particular pressure. On a simplistic level the freezing of liquid water to solid ice can be thought of as a loose analogy to explain sub-cooling. When water is cooled to just below 0°C, it does not freeze instantly, but with time it will eventually become a solid. The lower the temperature is below freezing point of water (the higher sub-cooling), the faster the ice will form. The same is true for hydrate formation; the rate of hydrate formation is a function of sub-cooling or the difference between the actual fluids temperature and the thermodynamic hydrate formation temperature. The sub-cooling and induction time applies when the system sits between the dissociation curve and nucleation curve.

The nucleation curve is also shown in Figure 4; anywhere left of the curve hydrate form instantly since the driving force or subcooling is met. Nucleation can occur when a system sits between the dissociation curve and nucleation as well but is considered a stochastic behaviour not just temperature and pressure dependant [6]. Thus, depending on design situations it may be possible that dissociation curves are generated conservatively.The PVT package MultiFlash used in this work contains a hydrate nucleation model developed in collaboration with BP (as part of the EUCHARIS joint industry project) [6]. In this model the nucleation point is described as the point where hydrate can realistically form instantly, based on statistical theory of nucleation in multicomponent system, and an accuracy of ±2°C when compared to the experimental data it was derived from [6].

Within oil, gas and water systems there are other factors that can influence the kinetics of hydrates formation such as natural inhibitors. This can include salts in the produced water and organic make-up of a particular oil, which is more less field specific [7]. Nucleation of hydrates is important to understand when examining transient scenarios. The driving force for nucleation includes the degree of sub-cooling and how long it has been subcooled [8].

Turner [9] described theorized hydrate formation mechanisms during a cold restart of an oil and gas production flowline. This included nucleation as discussed above, and mass transfer and heat transfer limitations. Mass transfer limitations occur because hydrate formation is an interfacial phenomenon and can be described as when hydrate is formed it can block or act as a wall at the interface of more water/gas molecules, limiting the mass transfer. Heat transfer limitations can be caused due to the exothermic nature of hydrate formation; as the hydrate formation starts to release heat and reversing the formation mechanism, at low sub-cooling this effect is greater as the released heat can counter how fast the system is cooling [9].

Kinnari [10] proposed a “hydrate management” technique adopted by an offshore oil and gas operator. The approach is based on a risked based approach considering the intrinsic properties of a fluid system, the hydrodynamics, and the plugging risk related to water present. The analyses results in an induction time plot for the specified oil systems, outlining timing on risk of hydrate occurances. This can extend operational time windows. Figure 5 illustrates the induction time concept as Kinnari calls it “hydrate kinetics technology” [10].

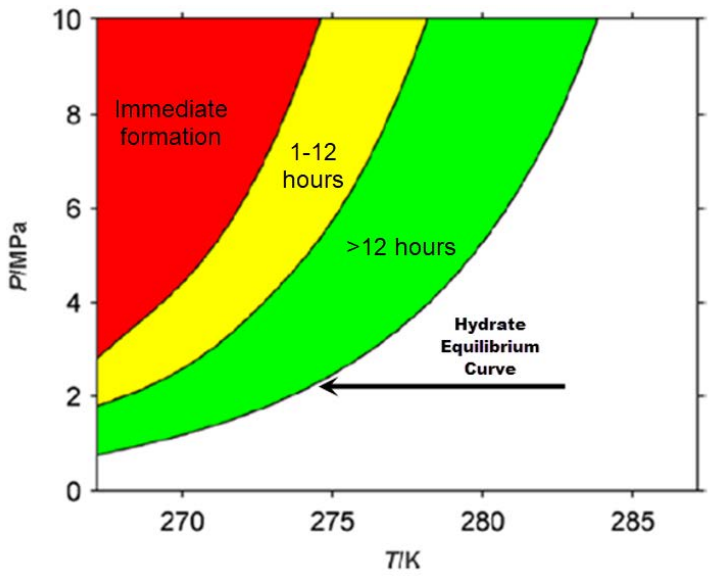

Figure 5: Kinnari typical oil system induction plot **[10]**

The plot is based on an experimental study for a specific oil where the green zone induction time is longer than 12 hours, the yellow zone 1-12 hours, and red represents immediate formation [10]. This supports that some degree of sub-cooling from a dissociation point can be acceptable in guiding an operating field's philosophy.

Bringing this understanding of hydrate formation forward, it shows that design on the basis of a hydrate dissociation curve in some cases can prove conservative and costly. As offshore development extends to longer distance and as fields mature, having tools for engineers to guide philosophy can be advantageous, rather than simplistically staying to the left of a hydrate dissociation curve at all times. Any situations when dealing with hydrate potential must come with caution and requires robust consideration but having tools for such consideration can be proven to be a worthwhile investment. More modern research has been taking it a step further to the understanding of the hydrate formation phenomenon, is centered around preventing hydrate blockages rather than preventing the formation of hydrate [11].

2.2 Study Approach

The first part of this study identifies the modeling tools in order to replicate real field scenarios. A multiphase dynamic simulator called OLGA with an attachment module called CSMHyK is selected. The next sections of this Chapter (2.3 & 2.4) will describe these models.

OLGA models are built with details of field architecture and fluid models within Chapter 3.0. The fluid models describe phase behaviour, attributes inputed to flow/thermal models, and thermodynamic hydrate dissociation/nucleation curves. These fluid models are built with Multiflash, which is the fluid properties software included with the OLGA software package.

Real field situations are identified where either a hydrate had formed (Chapter 4.0) and where hydrate formation was considered a risk (Chapter 5.0). All data related to these situations

was collected related to pressure, temperature, and fluid measurement in order to understand what was actually occurring within the system.

The conditions of interest that occurred within the field situations are re-modeled using the OLGA models connected with the kinetic model to describle the reaction rate of hydrate formation. Finally the results are assessed based on the predicted hydrate formation. Figure 6 is a simple flow diagram to describe this approach.

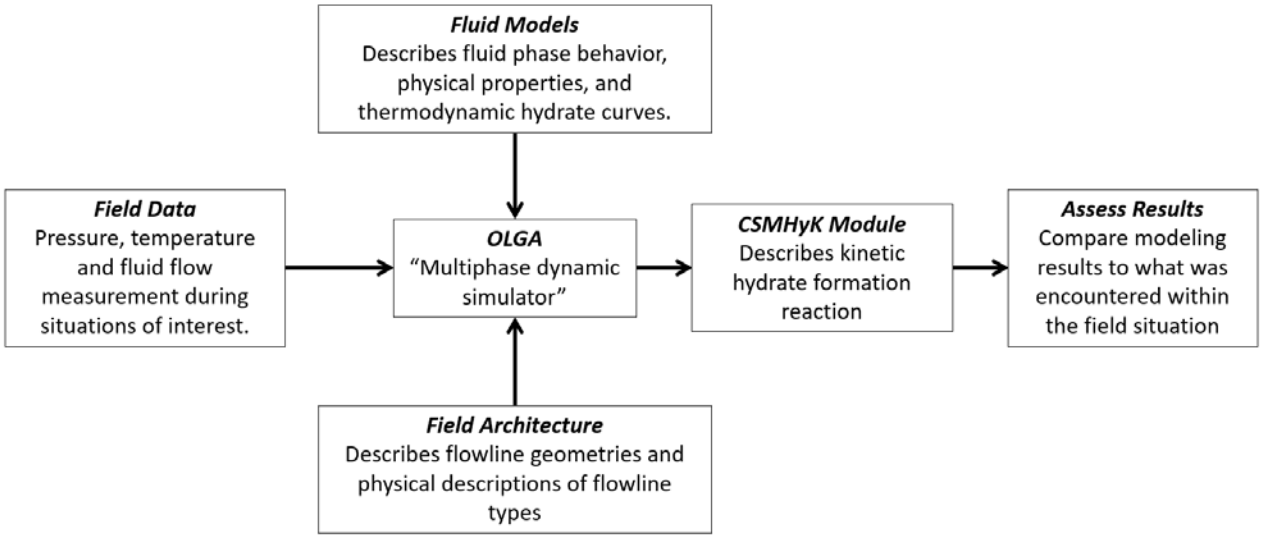

Figure 6: Study Approach

2.3 Introduction to OLGA and modeling capacity

The OLGA software tool is a transient multiphase flow simulator. The name OLGA is short for "oil and gas simulator". It can predict pressure drop, flow regimes, and thermal behaviour dynamically and since most of the time the multiphase flow is dynamic, it can be a powerful tool rather than depending on steady state calculations. It is the highest regarded multiphase simulator within the oil and gas industry used for design. The development of OLGA started in 1979 with the first code written in 1980 [12]. The early versions of OLGA were based upon many empirical correlations but was later updated to become a more mechanistic model based upon fundamental physics to improve from laboratory scale to field scale [12] [13].

OLGA is a one-dimensional simulator; basically geometry is created to represent a pipe broken into pipe volume sections to model the flow of hydrocarbons. Transport equations for mass, momentum and energy act as the foundation for the modeling engine [14]. Thermal effects are also robustly simulated by calculating the inner wall heat transfer coefficient based upon the fundamental heat transfer mechanisms of conduction, convection, and radiation with good accuracy [14].

Figure 7 illustrates how a pipe segment is broken into boundaries and section volumes. Each pipe volume is solved dynamically using the transport equations for pressure, temperature, flowrates, flow regime, and fluid composition. Boundary conditions at each side of the pipe

are specified. The fluid composition is specified using a PVT model along with the pipe characteristics and materials. Figure 8 is a summary diagram of OLGA modeling engine. The CSMHyK model is applied to each volume section in transient time of a pipe to estimate hydrate formation when water/gas exist together in the system. This hydrate kinetics model is described in the next chapter.

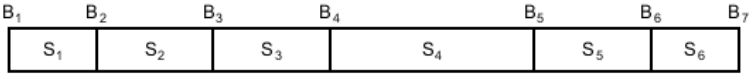

Figure 7: Pipe segment broken into boundaries and volume sections **[14]**

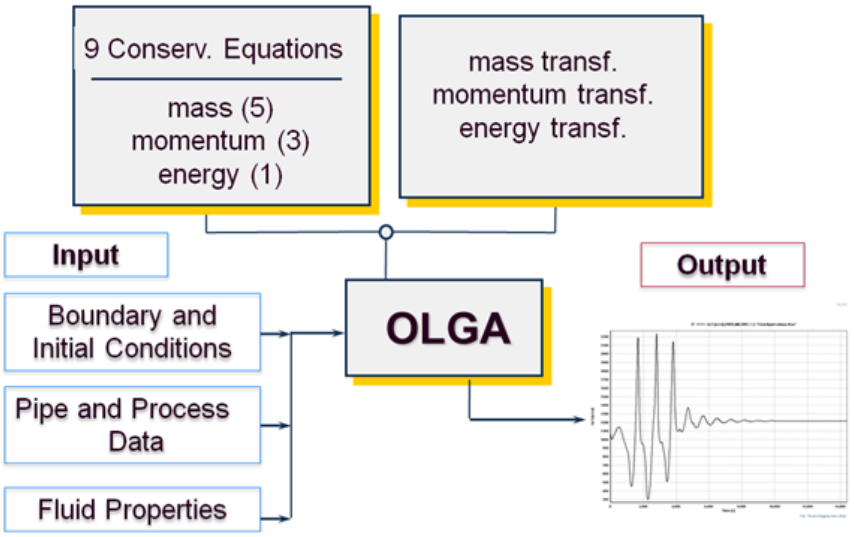

Figure 8: Main components of OLGA Model **[14]**

2.4 Colorado School of Mines Hydrate Kinetics Model (CSMHyK)

In 2002 the Deepstar Initiative (a group of oil and gas operators with the purpose of evolving technology) formed to discuss hydrates during production and agreed that they have operated pipelines under risky conditions in which a hydrate could form. As a result, a need for a better tool was recognized and joint effort was initialized which has resulted in Colorado School of Mines Hydrate Kinetics model (CSMHyK) [15] [16].

CSMHyK is a comprehensive transient hydrate model that predicts the behaviour of hydrate formation and its transportability [17]. The goal of CSMHyK is to predict where and when hydrate plug will form in a flowline during transport [17].

The hydrate kinetics model (CSMHyK) is the result of over a decade of work at the Colorado School of Mines [17]. The model is based upon the premise that hydrates form at the interface of water droplets and the oil phase which can then agglomerate to cause blockages [17] [9]. Within the model this is treated as slurry. The viscosity increases as the agglomeration grows [17]. This mechanism is illustrated in Figure 9. The current model assumes oil-dominated system with ongoing efforts to account for water and gas dominated systems.

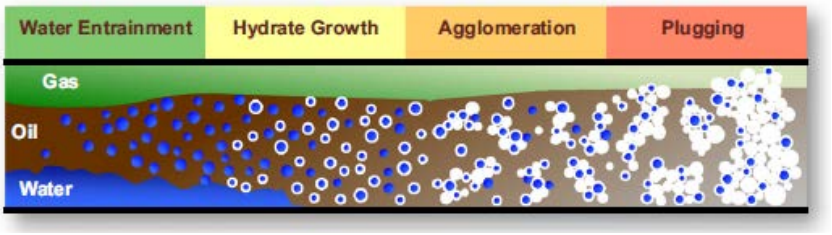

Figure 9: Conceptual model basis for CSMHyK **[17]**

The model includes intrinsic hydrate kinetics equation, mass and heat transport equations for hydrate formation, and a cold flow model for stabilized slurry flow [17]. An assumption is made to when hydrates form within the kinetics equation in terms of the sub-cooling to initiate the hydrate formation. A thermodynamic hydrate dissociation curve is inputed to the model based on the gas composition of interest. This is used as the basis as to when enough subcooling is reached within the system, the kinetic hydrate reaction starts. The model has been tested, tuned, and validated within the flow loop facilities to confirm the appropriate rate of hydrate formation rate [18]. The model allows for a real estimation of how fast hydrate may form within a flowline accounting for limitations in terms of mass and heat transfer resistances. Experimental validation of the model has been performed in flow loops. There is currently very little validation from actual field experience. The flow loop tests are considered experimental means of validating the modelling results under properly controlled test environments [19].

This work will analyze the results of CSMHyK based upon applying it to existent oil field situations. Capabilities of OLGA as discussed in the previous chapter make it a logical choice to couple with the transient hydrate formation model. It focuses on the volume fraction of hydrate predicted to form, not necessarily if the model says it plugs or not since this is more complicated. Knowing the predicted volume fraction that can potentially exist within subsea flowlines is a step towards enabling better informed decisions within the operation and

design conditions, rather than relying solely on a hydrate disassociation curve. This is especially important in start-up and shut-down scenarios.

3.0 Modeling Methodology

3.1 Overview

The methodology behind this modeling within the study will be presented in this section which includes:

1. Modeling of field's fluids PVT properties such as phase behavior, densities, and viscosities based on lab data
2. Modeling of hydrate curves including a comparison to lab testing data
3. Set up of physical OLGA models for each case

3.2 Fluid Model

MultiFlash is utilized as the phase behavior properties engine to input into the OLGA model. Two methods can be utilized to feed fluids properties to an OLGA model, which includes generating tabular fluid property files or compositional tracking. Tabular fluid property tables include the fluid properties generated by MultiFlash using a PVT model. OLGA reads this table for the particular conditions (pressure & temperature) within a system and uses that for the multiphase calculations. This may include interpolation between values on the table of properties. This is well suited to simulations that don't have significant phase changes throughout a simulation. In the Compositional tracking (CompTracking) model the phases compositions are calculated based on equilibrium flash modelling set up in the MultiFlash file and tracked throughout the OLGA model based on which at the pressure and temperatures of the flowline in each pipe segment, the fluid properties are also calculated.

The fluid model to feed properties to the OLGA flow model is based on laboratory experiments on bottom hole samples collected at reservoir temperature and pressure from a delineation well, which has historically been relied on for representative fluid properties.Laboratory tests that were conducted for the fluid of interest include:

- Compositional Analysis
- Bubble point measurement
- Differential Liberation testing
- Viscosity Measurement

The compositional analysis results presented in Table 1 are based on the sample of interest:

Table 1: Compositional analysis of field hydrocarbons **[20]**

Component	Mole Fraction
NITROGEN	0.54
H2S	0
CO2	1.04
METHANE	48.83
ETHANE	4.2
PROPANE	2.88
ISOBUTANE	0.52
N-BUTANE	2.13
ISOPENTANE	0.88
NEOPENTANE	0
N-PENTANE	1.11
C6	1.6
METHYLCYCLOPENTANE	0.58
BENZENE	0.15
CYCLOHEXANE	0.87
C7	3.03
METHYLCYCLOHEXANE	0.05
TOLUENE	0.32
C8	1.98
ETHYLBENZENE	0.34
M-XYLENE	0.14
P-XYLENE	0.14
O-XYLENE	0.28
C9	2.06
C10	1.96
C11	1.87
C12	1.65
C13	1.84
C14	1.50
C15	1.39
C16	1.30
C17	1.18
C18	1.14
C19	1.01
C20	0.93
C21	0.80
C22	0.77
C23	0.67
C24	0.60
C25	0.58
C26	0.47
C27	0.49
C28	0.49
C29	0.42
C30+	5.1

Other relevant properties with regards to the phase behavior tuning based on lab data include:

- Total molecular weight = 108.58
- Oil stock tank density = 28.7° API (883 kg/m^3 @ 15.6°C)
- Bubble point = 29,151 kPa @ 106°C

The composition is used as the basis to tune the phase behaviour modeling within the MultiFlash software for the phase behaviour model input to OLGA. The chosen equation of state (EOS) to characterize the PVT data was Peng-Robinson 1978 advanced version (PR78A) [21].

Table 2 summarizes the characterized composition after lumping the heavier components into pseudo components and tuning procedures carried out within the software [22]. This characetized fluid is also utilized to generate hydrate a hydrate curve in chapter 3.3.

Table 2: Tuned Fluid Composition Utilized for Modeling

Components	Mole Fraction
NITROGEN	0.54
CO2	1.04
METHANE	48.83
ETHANE	4.20
PROPANE	2.88
ISOBUTANE	0.52
N-BUTANE	2.13
ISOPENTANE	0.88
N-PENTANE	1.11
METHYLCYCLOPENTANE	0.58
BENZENE	0.15
CYCLOHEXANE	0.87
METHYLCYCLOHEXANE	0.05
TOLUENE	0.32
ETHYLBENZENE	0.34
M-XYLENE	0.14
P-XYLENE	0.14
O-XYLENE	0.28
C6-9	8.67
C10-14	8.40
C15-19	6.03
C20-29	6.15
C30+	5.57

Table 3 and Figures 10-13 summarize parameters for the PVT model compared to the laboratory data.

Table 3: Bubble Point & Density - Model vs. Lab results

Parameter	PVT Model	Lab Data
Bubble point @ 106°C (kPag)	29,180	29,150
Stock tank density of oil @ 15.6 °C (kg/m^3)	876	883

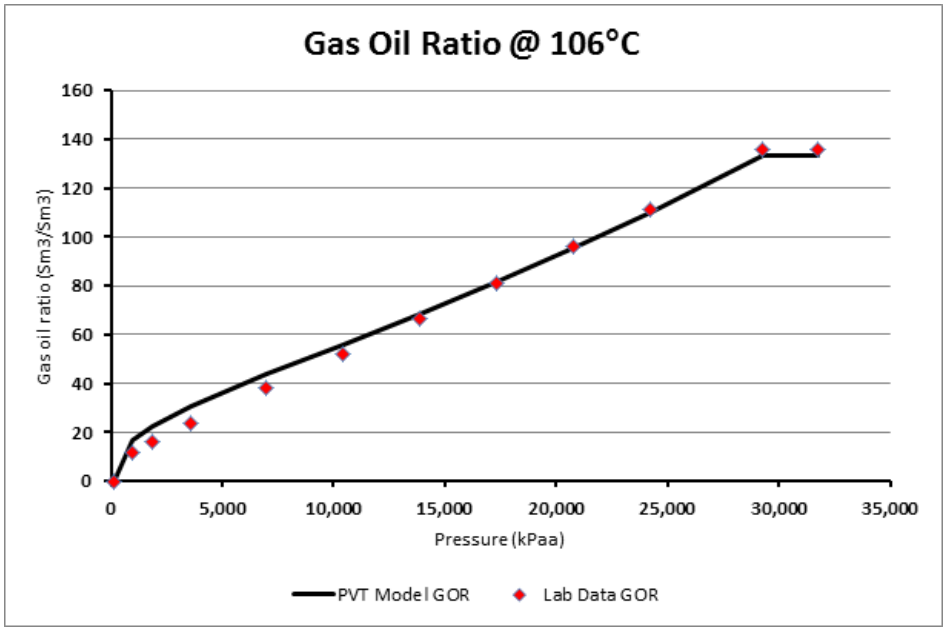

Figure 10: Gas Oil Ratio @ 106°C - Model Vs Lab

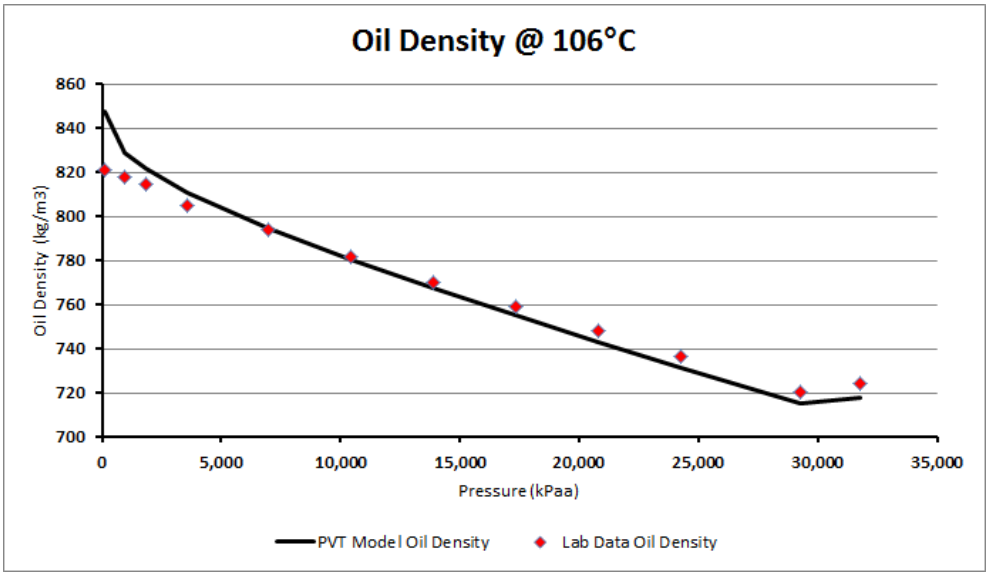

Figure 11: Oil Density @ 106°C - Model Vs Lab

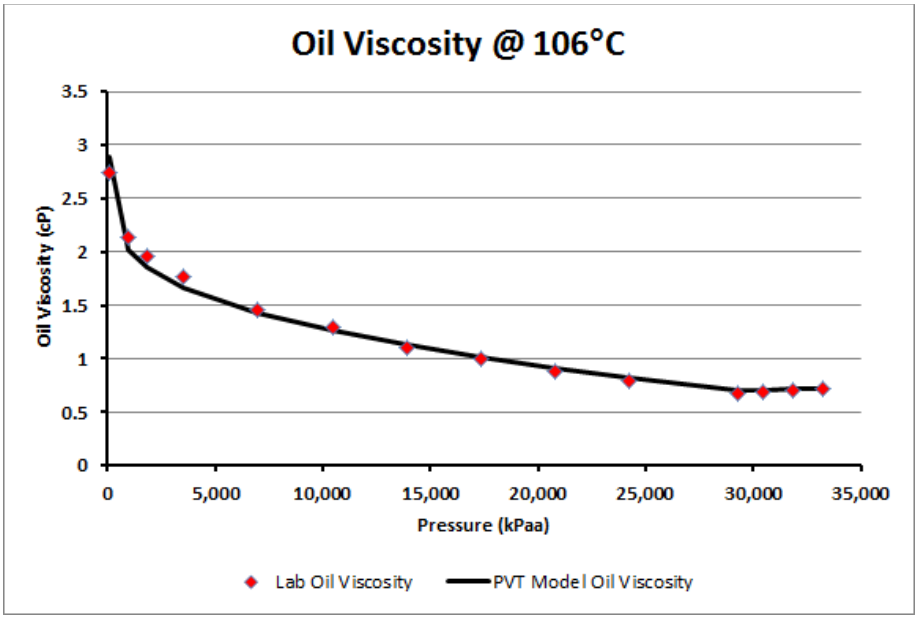

Figure 12: Oil Viscosity @ 106°C - Model Vs Lab

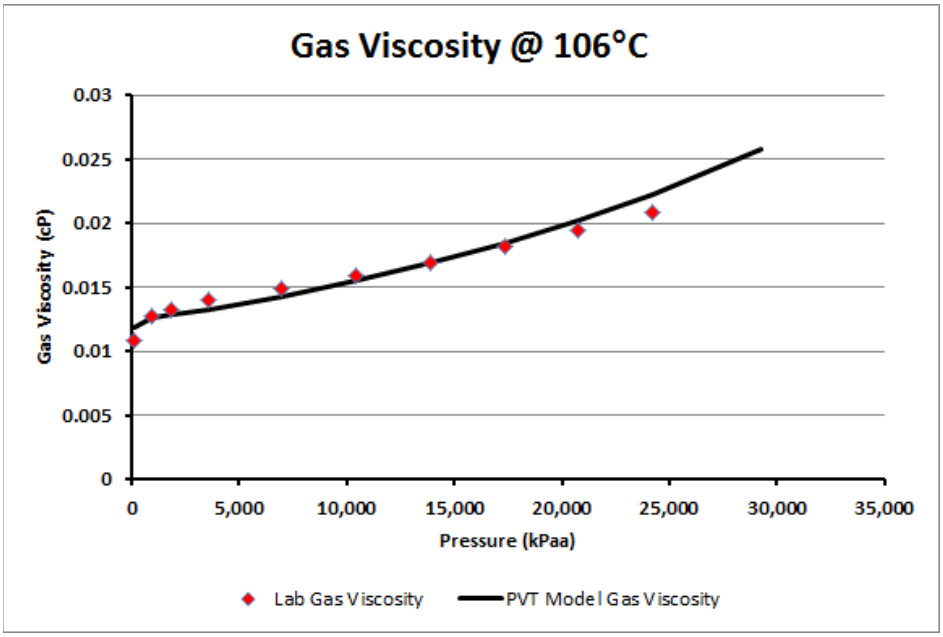

Figure 13: Gas Viscosity @ 106°C - Model Vs Lab

It can be seen that Figure 10 to Figure 13 illustrate the model predictions correspond well with GOR, phase densities, and phase viscosities.

3.3 Hydrate Dissociation and Nucleation Equilibrium Curves

An input within the simulation models includes the hydrate equilibrium curve in the form of a table. This table is required as a basis to be used in the model to predict the hydrate formation conditions of the fluids of interest. The two types of diagrams presented within the section are the hydrate dissociation curve and the hydrate nucleation curves.

The most common curve utilized within design consideration is the hydrate dissociation curve. To the left of the curves (towards lower temperature and higher pressure) is where hydrates are thermodynamically stable and to the right of the curves represent the area where hydrates do not exist as illustrated in Figure 4. A system can move from the right of the curve into hydrate risk zone however this does not necessarily mean that hydrate will form instantly, rather there is a potential for the hydrate to form. It is therefore very important to understand the kinetics of hydrates formation reactions as to how fast hydrate can form.

The hydrate nucleation curves represent when hydrate would theoretically form crystals instantly. The nucleation curve is based on the stochastic behaviour of how hydrate crystals form and provides an estimate of the condition that cause hydrate crystals to go from meta-stable to stable [6]. If a condition is sitting between the nucleation and dissociation curve, the risk of hydrate formation will be related to the time scale and kinetics of the hydrate formation process [6]. The nucleation model utilized within MultiFlash was developed with BP as part of the EUCHARIS joint industry project and it is suggested the error band of the model is +-2°C [6]. To generate hydrate nucleation and dissociation curves, the MultiFlash software is utilized; the composition of the downhole sample from the previous chapter 3.2 and the dehydrated injection gas for the field are shown in Table 4. The dehydrated injection gas is based on samples routinely taken through the topsides process; this gas is used within all the wells in the field as the lift gas.

Table 4: Dehydrated Injection Gas Composition **[23]**

Component	Mole Fraction
NITROGEN	0.31
CO_2	2.73
METHANE	85.14
ETHANE	5.9
PROPANE	3.55
ISOBUTANE	0.45
N-BUTANE	1.03
ISOPENTANE	0.26
N-PENTANE	0.32
C_6	0.2

Figure 14 shows hydrate curves generated that are relevant to the field of interest. The green "Lift Gas Hydrate Dissociation Curve" is used in all models of this study coupled with the CSMHyK model as discussed in chapter 2.4.

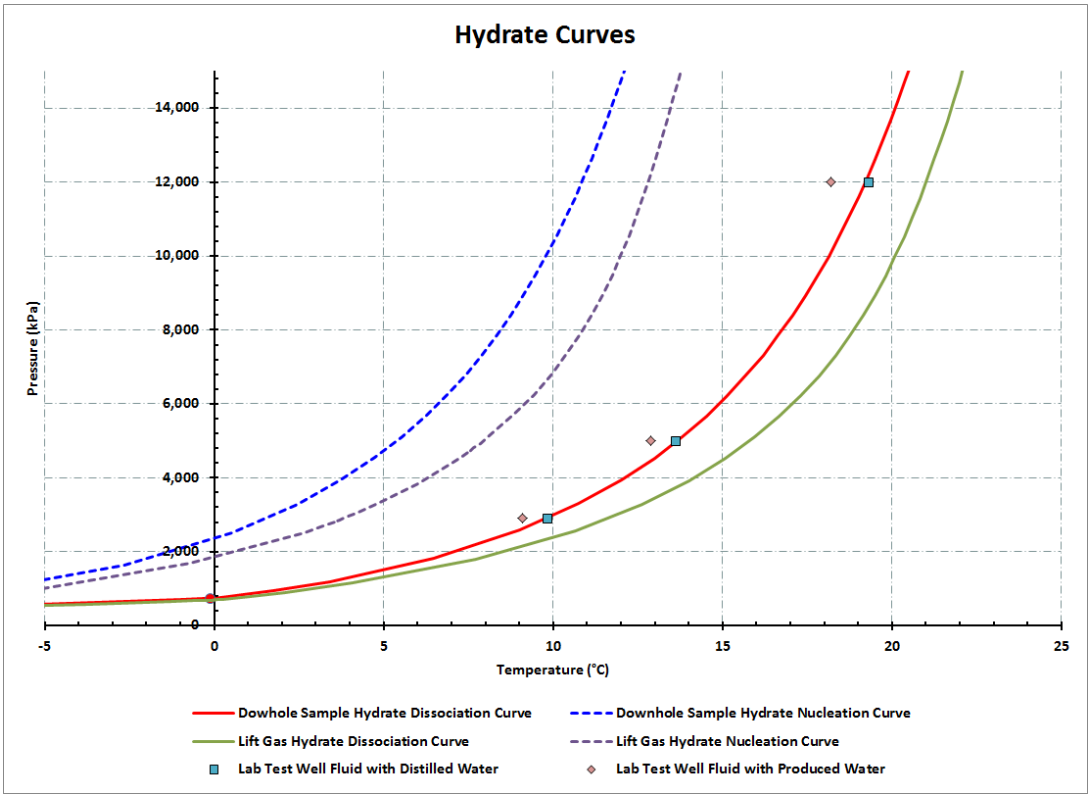

Figure 14: Hydrate curves relevant to analysis

Laboratory testing data from previous work is also plotted to demonstrate the validity of the thermodynamic models behind the hydrate curves [24]. For the purpose of this analysis the lift gas hydrate dissociation curve was used as the input to the modeling software. This may also be conservative in ways but theoretically when a flowline is shut with hydrocarbons and water, there could be potential for predominantly water and lift gas to co-exist. Figure 14 also shows test points using gas from topsides against distilled water and produced water (containing salts). The impact of the composition of the produced water can shift the curve to the left due to the salts (salting out), but in this case it is not significant. Figure 15 is a visualization of experimental lab work showing the hydrate dissociation points [24].

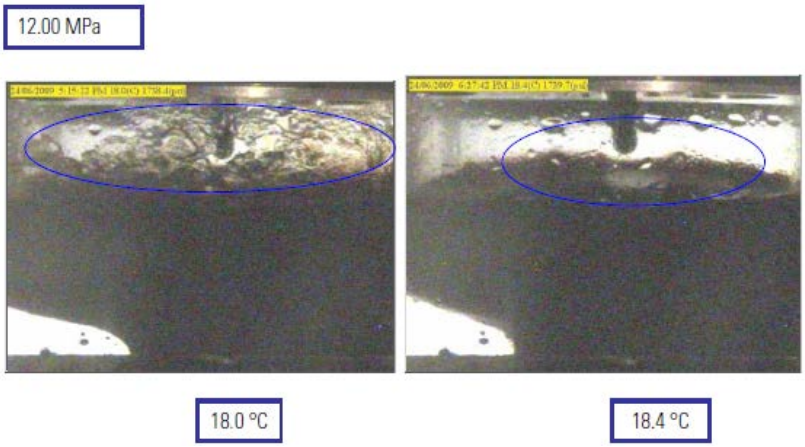

Figure 15: Hydrate experiment on field fluids (produced water case) **[24]**

It can be seen in Figure 15 when the temperature is increased slightly the hydrate crystals on the surface are dissociated. Note that in these experiments the fluids were sub-cooled deeply within a PVT cell, then the system temperature was gradually raised to find the dissociation point.

3.4 OLGA Simulation Models

In this section the setup of the OLGA models will be discussed and presented. As discussed in chapter 2.3, the OLGA software models the flow of all the phases (oil, water, and gas) with respect to pressures and temperatures. The geometries of the flowlines and the wall structures for heat transfer purposes need to be represented. The next two sections of this chapter discusses the model setup for the two particular scenarios considered in this work. All flowlines and pipes are assumed to be surrounded by seawater with an ambient temperature of -1.8 °C with a sea floor current velocity of 0.94 m/s.

3.4.1 Rigid Production Spool

Within the subsea oil wells of this particular field, the production from the wells are connected from the tree to the manifold by a rigid spool. The spool is 6” (Inner diameter = 124.1 mm) rigid pipe and approximately 35 meters long. Figure 16 illustrates the geometry/elevations of the rigid production spool along with pipe representing the tree and manifold for the OLGA model. Details of the pipe wall utilized are shown in Table 5.

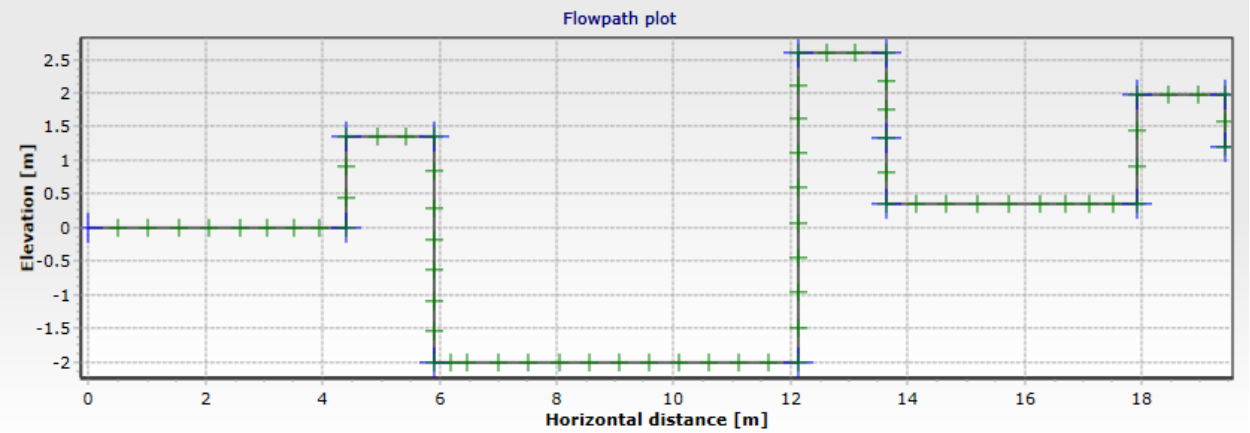

Figure 16: Rigid Spool Geometry

Table 5: Rigid Spool Wall Details

Material	Thickness (mm)	Thermal Capacity (J/kg-°C)	Conductivity (W/m-°C)	Density (kg/m^3)
Duplex	21.95	480	14.4	7600
SPU	55	1700	0.135	700

The boundary conditions for the model include the mass rates of oil/gas/water from the wellhead and the flowline pressure. Figure 17 illustrates the OLGA graphical user interface (GUI) view of the model. Chapter 4.0 applies real boundary conditions along with examining a actual hydrate blockage formation within this rigid spool model.

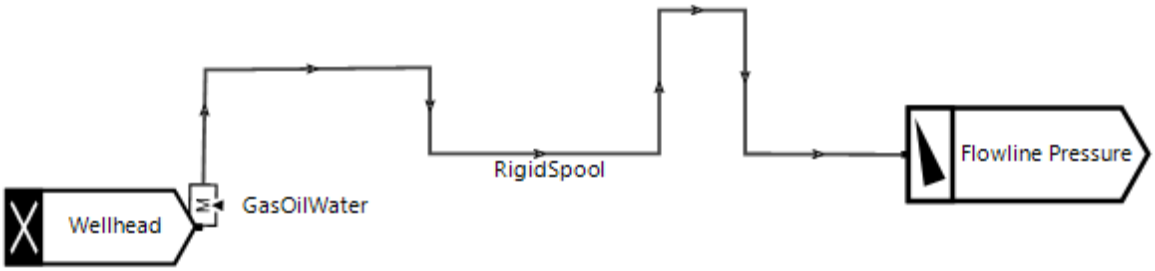

Figure 17: OLGA GUI of Rigid Spool Model

3.4.2 Production Flowline Field Model

This chapter describes the OLGA model for the flowline architecture that connects the production wells to the processing facility. Figure 18 represents the general layout of the production system of the producing field with three drill centers. The drill centers are where the production wells are located then tied back to the FPSO via the main flowlines. Figures

18 to 26 illustrate the geometries, including lengths and elevations, utilized within the OLGA model for each segment.

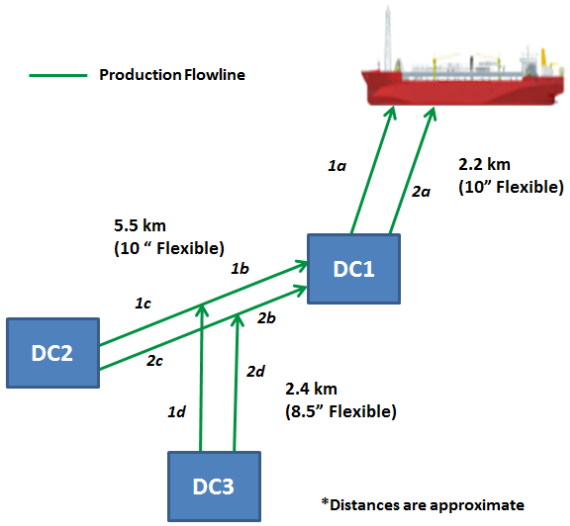

Figure 18: Overall Production Flowline Layout

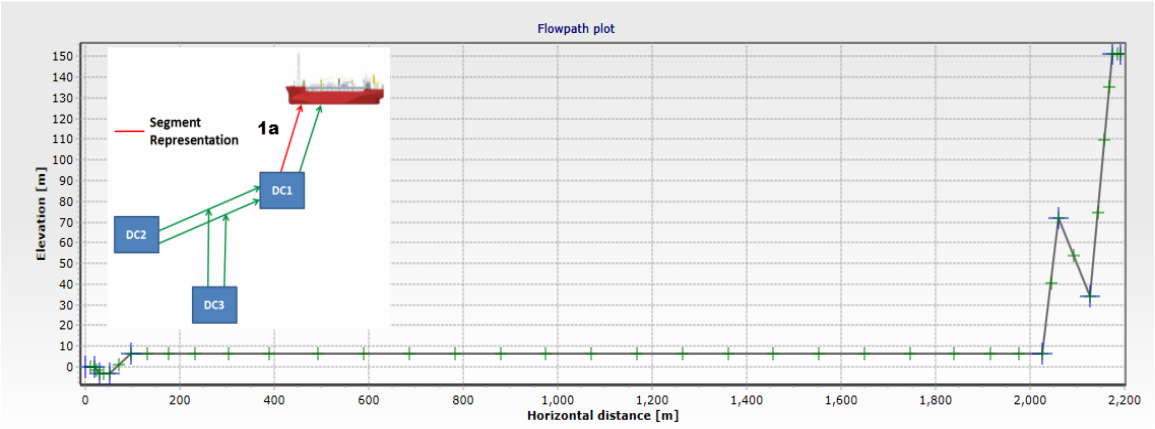

Figure 19: Flowline 1a geometry

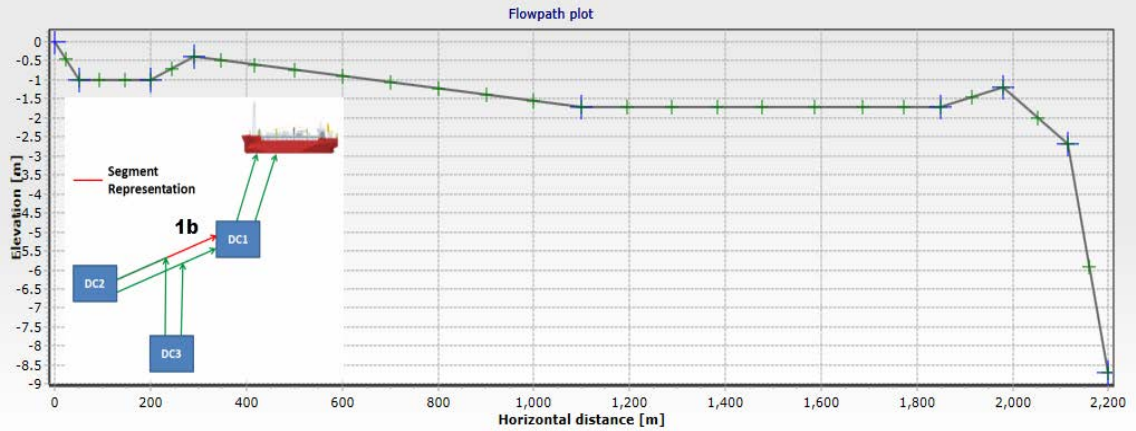

Figure 20: Flowline 1b geometry

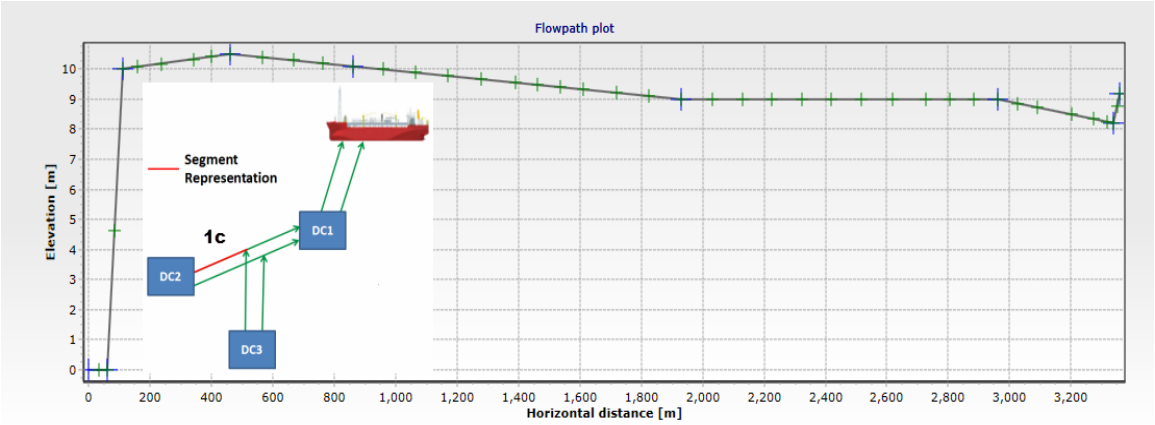

Figure 21: Flowline 1c geometry

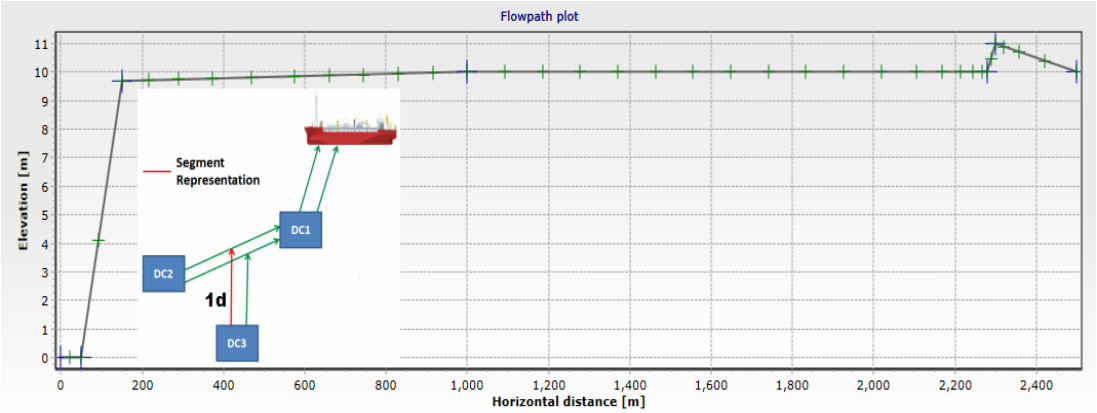

Figure 22: Flowline 1d geometry

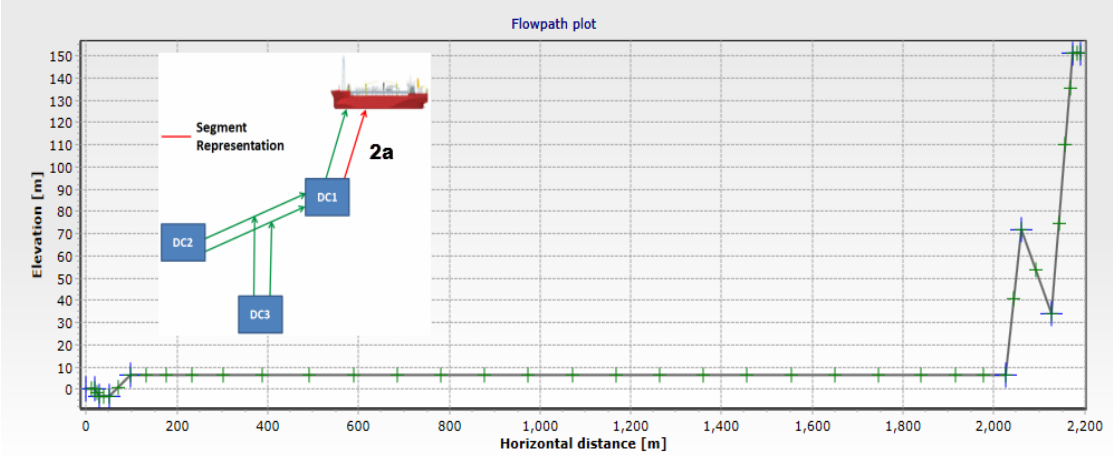

Figure 23: Flowline 2a geometry

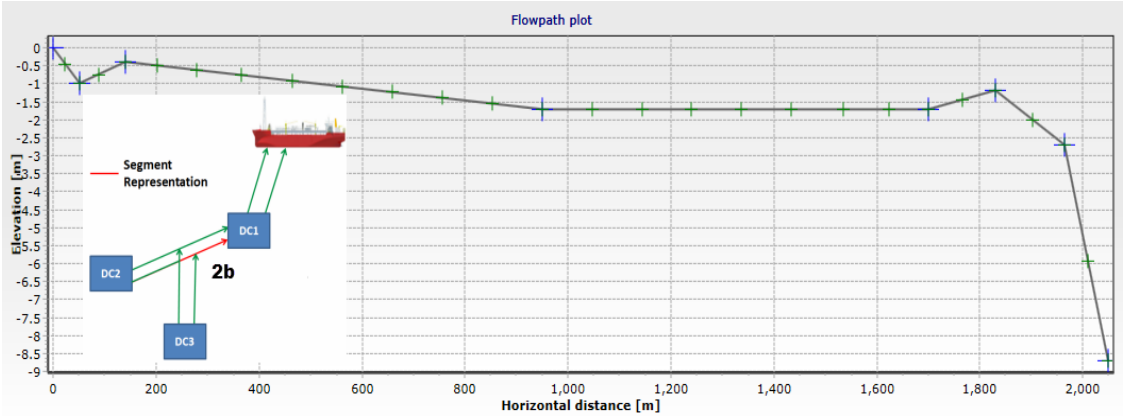

Figure 24: Flowline 2b geometry

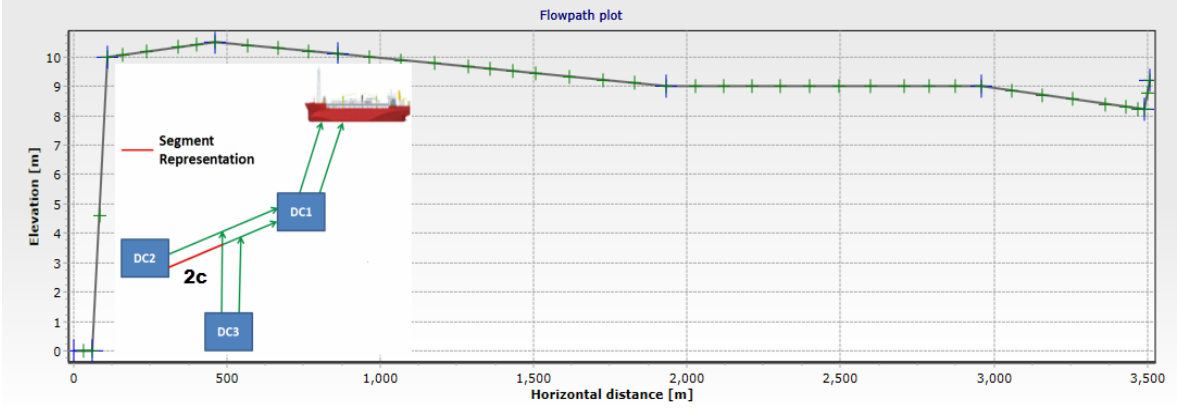

Figure 25: Flowline 2c geometry

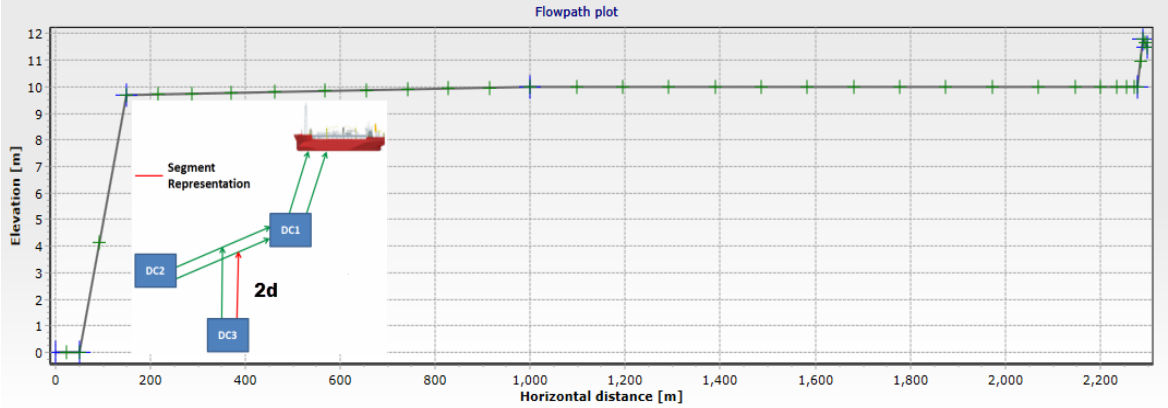

Figure 26: Flowline 2d geometry

The structures of the flexible flowlines are built within the software with the thicknesses and properties of each material for the overall heat transfer coefficient (OHTC) to be calculated within the simulations. Below is a summary of the wall structures for each flowline segment:

- Table 6: 10" Flexible Riser Wall Description – Last portion of segments 1a and 2a
- Table 7: 10" Original Flexible Flowline Description – Segments 1a and 2a
- Table 8: New 10" Flexible Flowline Description – Segments 1b, 1c, 2b, and 2c
- Table 9: 8.5" Flexible Flowline Description – Segments 1d and 2d

Table 6: 10" Flexible Riser Wall Description

Wall Layer Description	Thickness (mm)	Thermal Capacity (J/kg-C°)	Conductivity (W/m-C°)	Density (kg/m^3)
Carcass FE02	6.00	502.32	1161.65	4,800
Sacrificial/Pressure Sheeth Gammaflex	9.60	1500.00	0.1849	1,700
Zeta Wire FI 27	8.00	502.32	0.9300	7,850
Spiral FI 27	7.50	502.32	0.9300	7,850
Anti wear tape Polymid	1.50	2428.00	0.3350	1,040
Armour 1 FI 27	5.00	502.32	0.9300	7,850
Anti wear tape Polymid	1.50	2428.00	0.3350	1,040
Armour 2 FI 27	5.00	502.32	0.9300	7,850
Fabric Tape Ester	1.55	2511.60	1.1628	571
Riser External Sheath Rilsan TP08	9.30	2220.00	0.2000	1,010
Riser Protective ExtSheath Polyethylene TP14	9.70	2500.00	0.4070	950

Table 7: 10" Original Flexible Flowline Description

Wall Layer Description	Thickness (mm)	Thermal Capacity (J/kg-C°)	Conductivity (W/m-C°)	Density (kg/m^3)
Carcass FE02	6.00	502.32	1161.6500	4800
Pressure Sheeth Gammaflex	7.00	1500.00	0.1849	1700
Zeta Wire FI 27	10.00	1500.00	0.1849	1700
Armour 1 FI 27	5.00	502.32	0.9300	7850
Armour 2 FI27	5.00	502.32	0.9300	7850
Fabric Tape Prop	1.45	2511.60	1.1628	571
Intermediate Sheath Polyethylene TP04	8.70	2302.00	0.4070	955
Insulation MO1	11.00	1214.00	0.0605	730
Fabric Tape Ester	1.05	2511.60	1.1628	765
External Sheeth Polyethylene TP14	11.40	2500.00	0.4070	950

Table 8: New 10" Flexible Flowline Description

Wall Layer Description	Thickness (mm)	Thermal Capacity (J/kg-C°)	Conductivity (W/m-C°)	Density (kg/m^3)
Carcass FE02	6.00	502.32	1161.6500	4800
Pressure Sheath Coflon TP06	12.00	1480.00	0.1590	1747
Zeta Wire FI 27	10.00	1500.00	0.1849	1700
Sprial FI 27	7.50	502.32	0.9300	7850
Armour 1 FI 27	5.00	502.32	0.9300	7850
Armour 2 FI 27	5.00	502.32	0.9300	7850
High Strength Tape	2.55	2511.60	1.1628	571
Intermediate Sheath TP-Flex TP26	15.00	1805.00	0.2000	940
Insulation MO1	22.00	1214.00	0.1200	510
Fabric Tape Ester	0.50	2511.60	1.1628	765
Insulation	11.00	1214.00	0.1200	510
Fabric Tape G2 Ester	1.40	2511.60	1.1628	598
External Sheath Rilsan TP08	14.20	2220.00	0.2000	1010

Table 9: 8.5" Flexible Flowline Description

Wall Layer Description	Thickness (mm)	Thermal Capacity (J/kg-C°)	Conductivity (W/m-C°)	Density (kg/m^3)
Carcass	5.00	502.32	1161.6500	4800.00
Sacrificial/Pressure Sheath Gammaflex	9.10	1500.00	0.1849	1700.00
Zeta FI 27	8.00	1500.00	0.1849	1700.00
Sprial FI 27	5.00	502.32	0.9300	7850.00
First Fabric Tape	0.40	1479.40	0.6000	320.00
Armour 1 Layer FI 27	5.00	502.32	0.9300	7850.00
Second Fabric Tape	0.40	1479.40	0.6000	320.00
Armour 2 Layer FI 27	5.00	502.32	0.9300	7850.00
High Strength Tape	2.47	1863.16	0.5200	542.60
Insulation MO1	16.50	1214.00	0.1200	510.00
Third Fabric Tape	1.20	1627.60	0.6000	536.07
External Sheath TP-Flex TP26	9.40	1805.00	0.2000	940.00

Figure 27 illustrates the graphical user interface (GUI) within the final OLGA model developed based on the geometries illustrated above. The boundary conditions are also shown in Figure 27; where P1 and P2 represent the riser pressure and mass sources located at each drill center for the oil, water, solution gas, and gas lift (GL). Compositional Tracking option is utilized within the model; this feature allows the tracking of the composition throughout the flowlines and the thermodynamic and physical properties are calculated throughout the system. Within the mass source nodes; the mass flow rate and temperature of each fluid is defined. Chapter 5.0 applies real field data to this model in a situation when it was thought that hydrate conditions would have been present in sections of the production flowline system.

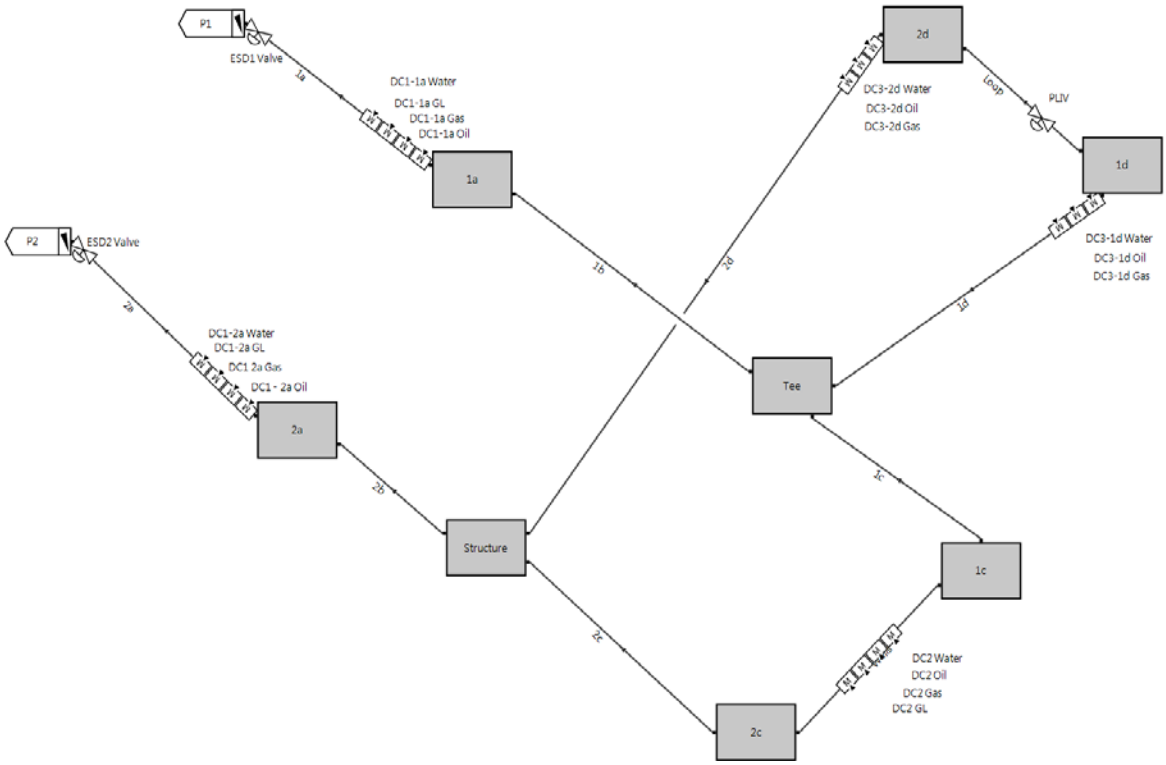

Figure 27: Field Model-OLGA Interface

4.0 Hydrate Plug within Rigid Production Spool

This section will focus on an event where a hydrate plug had formed a full blockage within a production spool which connects a mature oil well to the production manifold. It is a continuation of the model built within Chapter 3.4.1. The data from the occurrence is presented followed by modeling within the OLGA simulator and using the Hydrate Kinetics (CSMHyK) module.

4.1 Field Data – Hydrate Plug within Rigid Production Spool

The event of interest occurred when a well was deemed to be at the end of its life due to high water-cut and was shut-in with an untreated[1] production spool. Figure 28 is a picture of the samples taken off the test separator that represent of the well of interest. The well was shown to be producing little oil. This is also illustrated by laboratory tests to measure the oil content summarized within Table 10.

Figure 28: High water cut well samples

[1] Spools are treated with methanol to flush the lines off the reservoir fluids in a long shut down situations to prevent hydrate plug

Table 10: Summary of Lab Measurements for water content

Date	Time	Total Volume (mL)	Water Volume (mL)	Water Content (%)	Oil Content (%)
April 21, 2016	8:12 AM	495	494	99.8%	0.2%
April 21, 2016	8:13 AM	495	494	99.8%	0.2%
April 21, 2016	8:43 AM	499	496	99.4%	0.6%
April 21, 2016	8:44 AM	487	485	99.6%	0.4%
April 21, 2016	9:15 AM	494	490	99.2%	0.8%
April 21, 2016	9:16 AM	495	493	99.6%	0.4%
April 21, 2016	9:56 AM	491	485	98.8%	1.2%
April 21, 2016	9:57 AM	490	485	99.0%	1.0%
			Average:	99.6%	0.4%

Prior to shutting the isolation valves (tree wing or master valves) on the well, its Multiphase Flow Meter (MPFM) showed that the well was flowing approximately 600 Sm^3/d liquid and 7,000 Sm^3/d of gas. The general procedure to prevent hydrates after shutting in a well is to treat the wellbore and rigid production spool with methanol by flowing it from the tree. In this particular case, the hydrate prevention operation did not take place and was not realized until several months later. Due to the presence of gas and little oil it was concluded that a hydrate plug could have formed when the fluids stopped flowing and cooled down. Upon further investigation it could be seen that there was evidence of an exothermic reaction based on the MPFM temperature sensor. This is expected during hydrate formation reaction. Figure 29 and Figure 30 show the data from the MPFM.

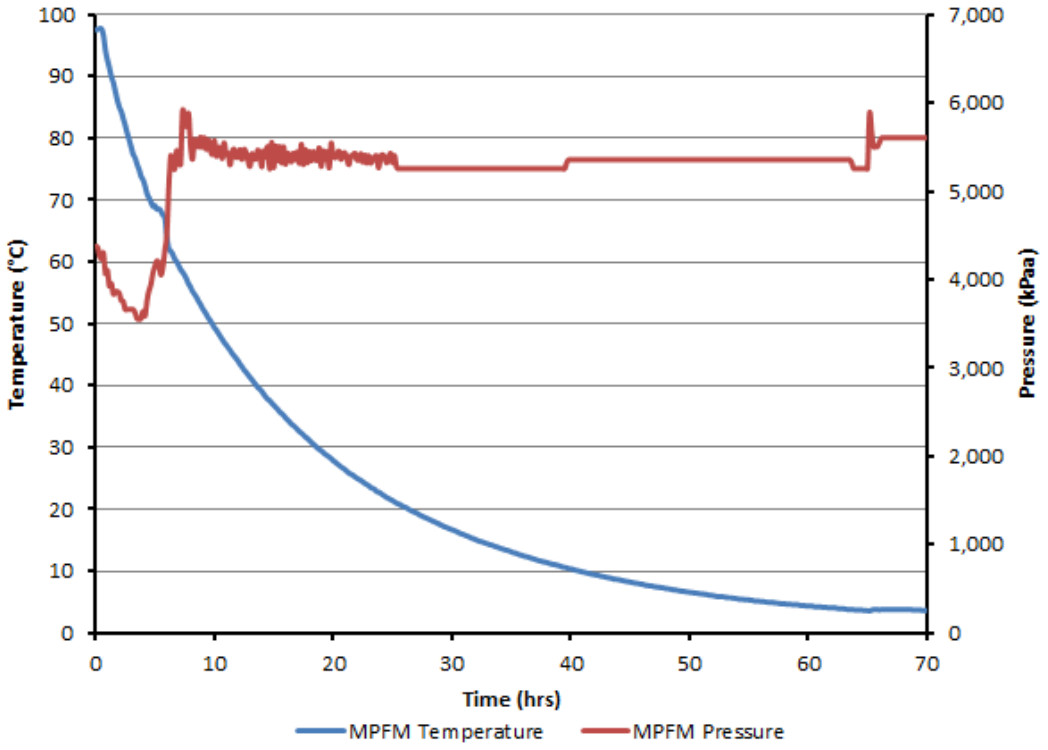

Figure 29: MPFM sensors showing cooldown of rigid spool

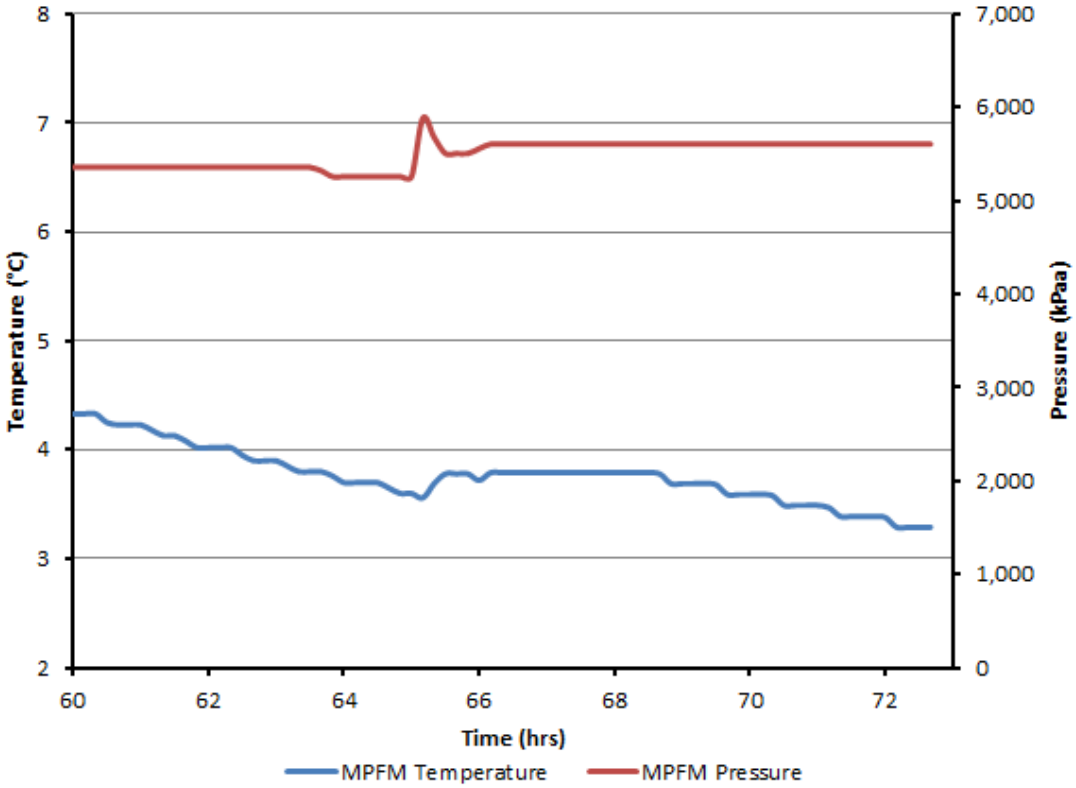

Figure 30: Close up of exothermic reaction evidence

At approximately 65 hours into the cooldown there was a slight pressure disturbance in the flowline (at this point the spool would have been a dead leg with the valve open to the live flowline) and the temperature increased approximately 0.5°C and stayed flat for approximately 3 hours before continuing to cool down. When the reaction started the temperature was approximately 3.5 °C and pressure was around 5,700 kPaa. This is an indication that the formation of hydrate actually took place approximately 35 hours after entering hydrate region on the dissociation curve at the particular point where the MPFM sensor is located. Note that there is likely some error on the MPFM sensors, the pressure was likely approximately 5,200 kPaa based on other sensors near this location. The approximate condition when the reaction started is shown on the hydrate curves in Figure 31.

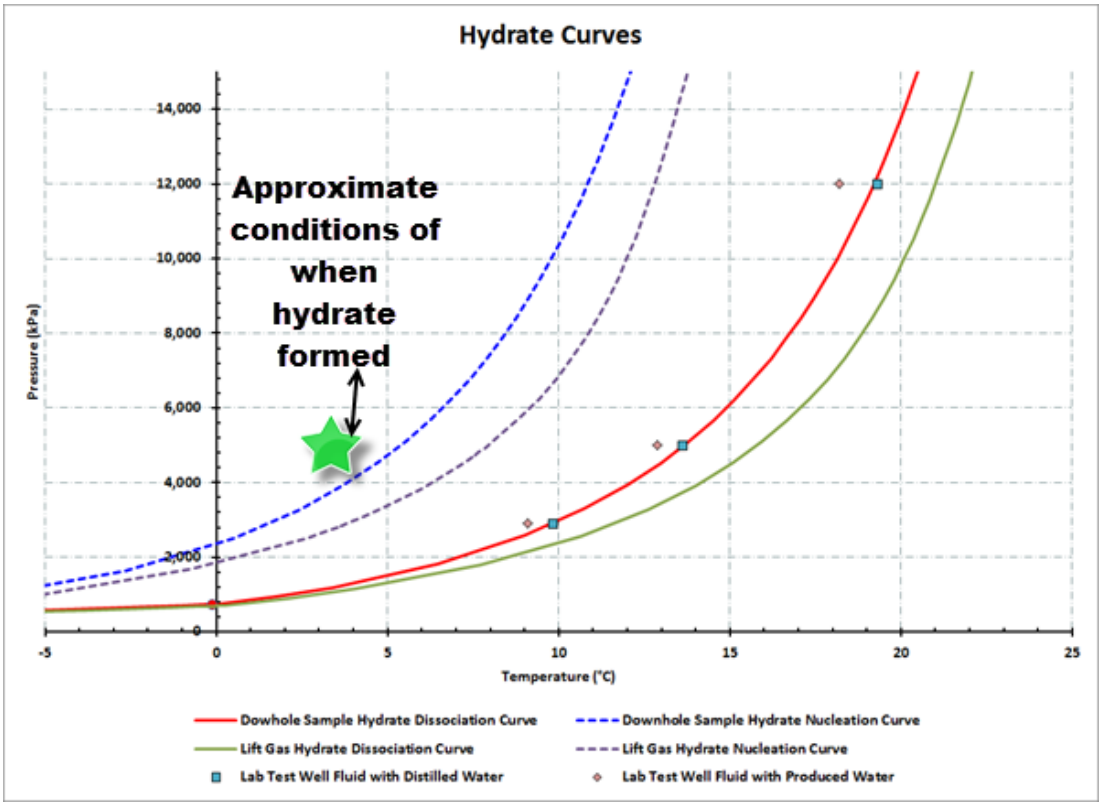

Figure 31: Hydrate curves and approximate condition of exothermic reaction

An operational program was run to check if a blockage had formed. An attempt was made to pump methanol through the tree and rigid spool towards the flowline. It was confirmed that there was a blockage in the spool based on the pressure sensors. Figure 32 shows the supporting field data and Figure 33 shows the corresponding location of the pressure reading on the rigid spool.

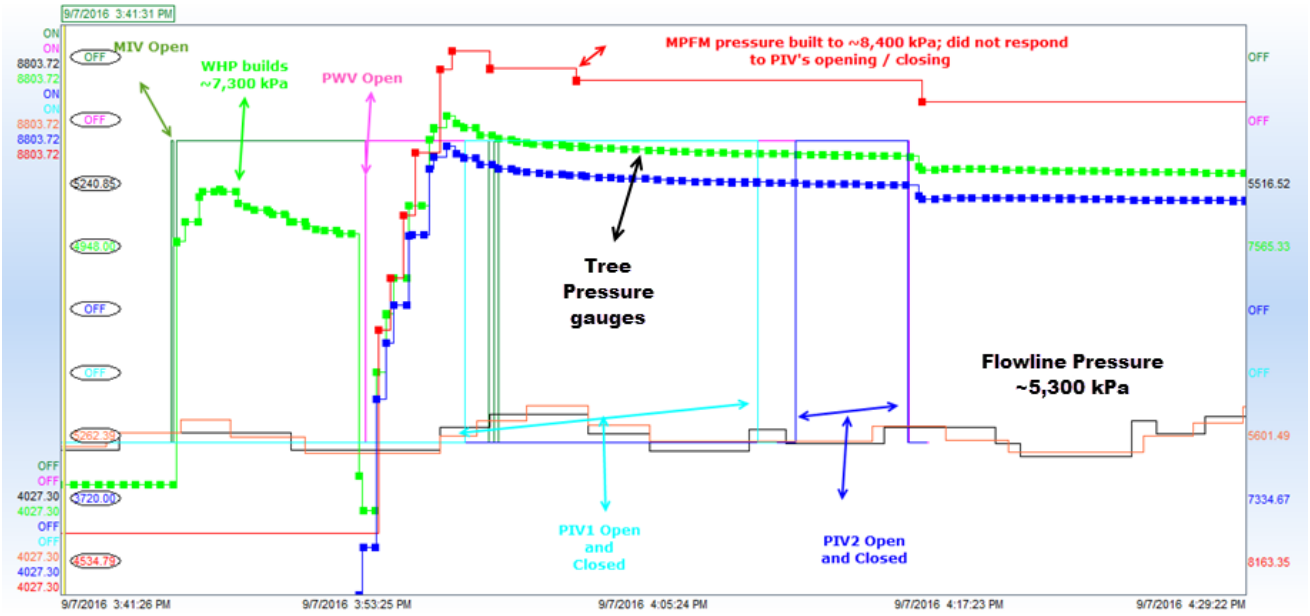

Figure 32: Rigid spool blockage data confirming blockage

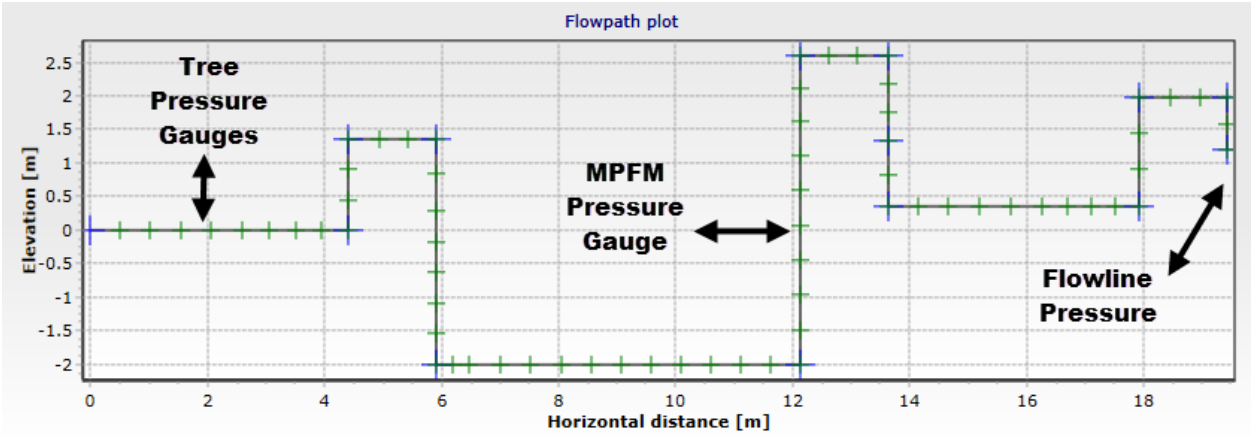

Figure 33: Approximant location of pressure readings

The field data shows that the methanol injection valve (MIV) comes open on the tree and the wellhead pressure builds after the production wing valve (PWV) is opened, in the attempt to push methanol through the rigid spool. Note that the production master valve (PMV) is closed in this case. Figure 34 is an illustration of the valving layout on a production tree. The tree pressure gauges and the MPFM pressure both showed pressure build up, which suggested communication from the tree out to the MPFM. The end of the rigid spool is open to flowline pressure which was around 5,300 kPa; this pressure is measured from other production trees. The pressure built within the spool towards 8,000 kPa confirming that a blockage was present. A subsequent remediation program was carried out safely and completed successfully by depressurization.

In the next section of this chapter, the actual conditions of when this blockage occurred is modeled using OLGA model coupled with the CSMHyK module.

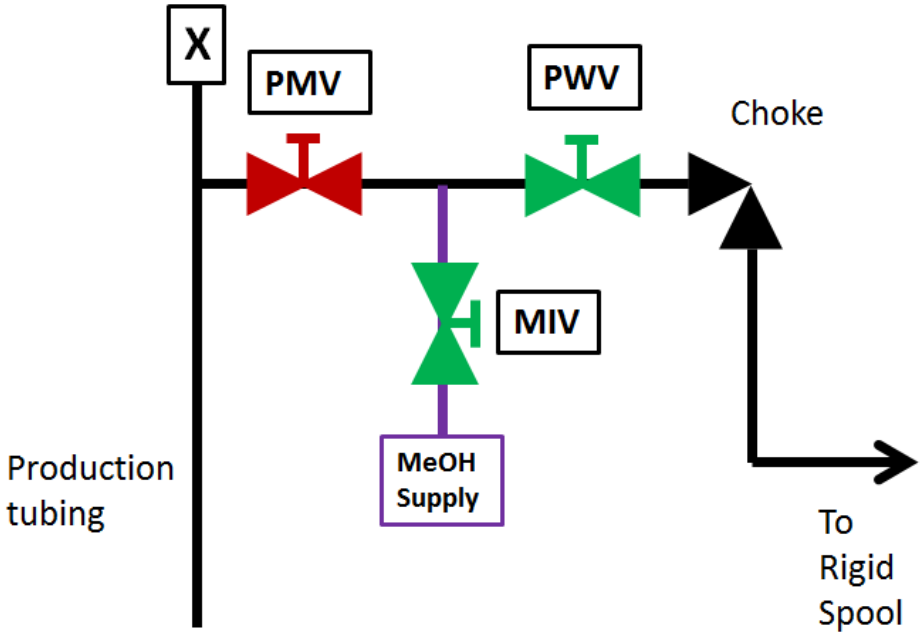

Figure 34: Tree valve layout

4.2 Hydrate Kinetic Model Results

This section outlines the results of the rigid spool blockage scenario modeling. The OLGA model is based on what was described in the sections with regards to fluid properties, geometries, pipe sizes, and conditions surrounding the scenario coupled with the Hydrate Kinetic module.

Figure 35 shows the actual temperature data from the MPFM within the rigid spool compared to the OLGA model at the positions for temperature trends picked within the model. Figure 36 illustrates the location of the temperature trends at the particular locations within the model geometry and also the location of the MPFM within the rigid pool. The predicted holdups with regards to liquid (HOL) and gas (AL) fractions within the dead rigid spool after shut-in are shown in Figure 37. It can be seen the high locations of the rigid spool is predicted to predominately be gas. It can also be seen that sections predicted to have gas cool down faster than the section predicted to have liquid. The general temperature trend sitting in the liquid holdup section agrees well with what seen at the MPFM.

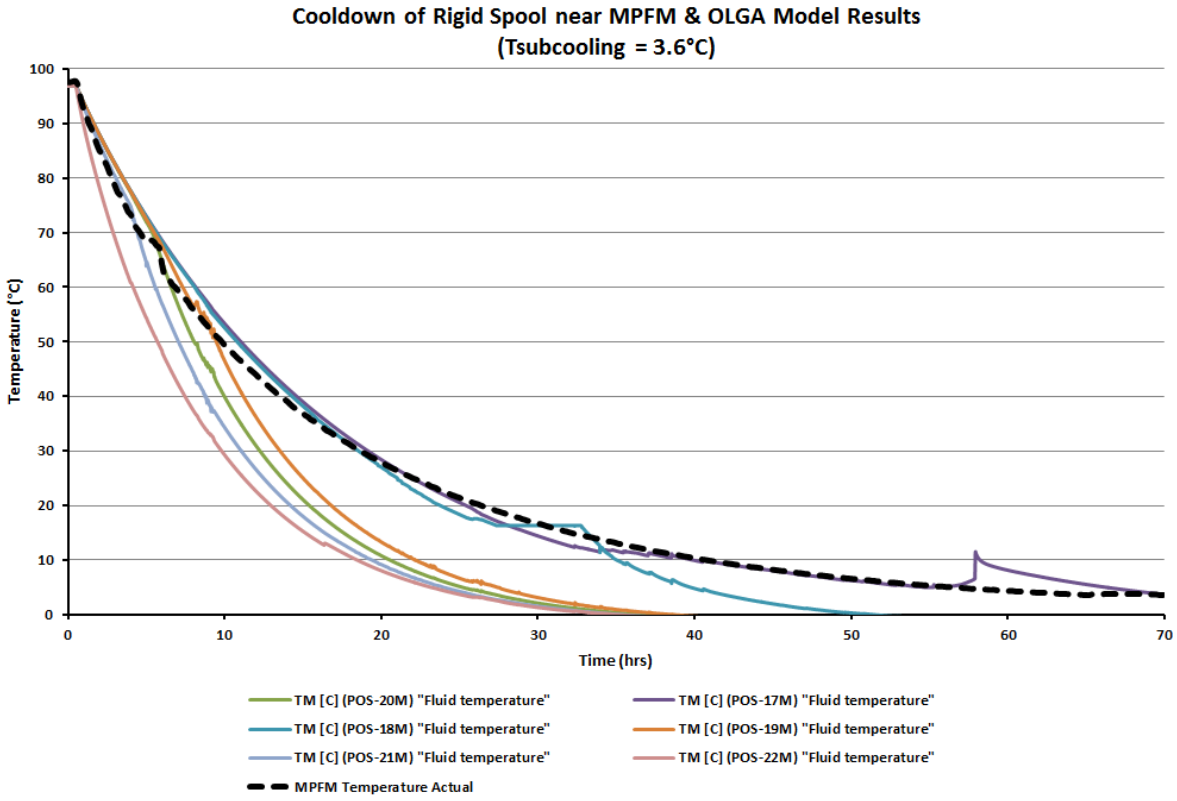

Figure 35: Cooldown of rigid spool near MPFM

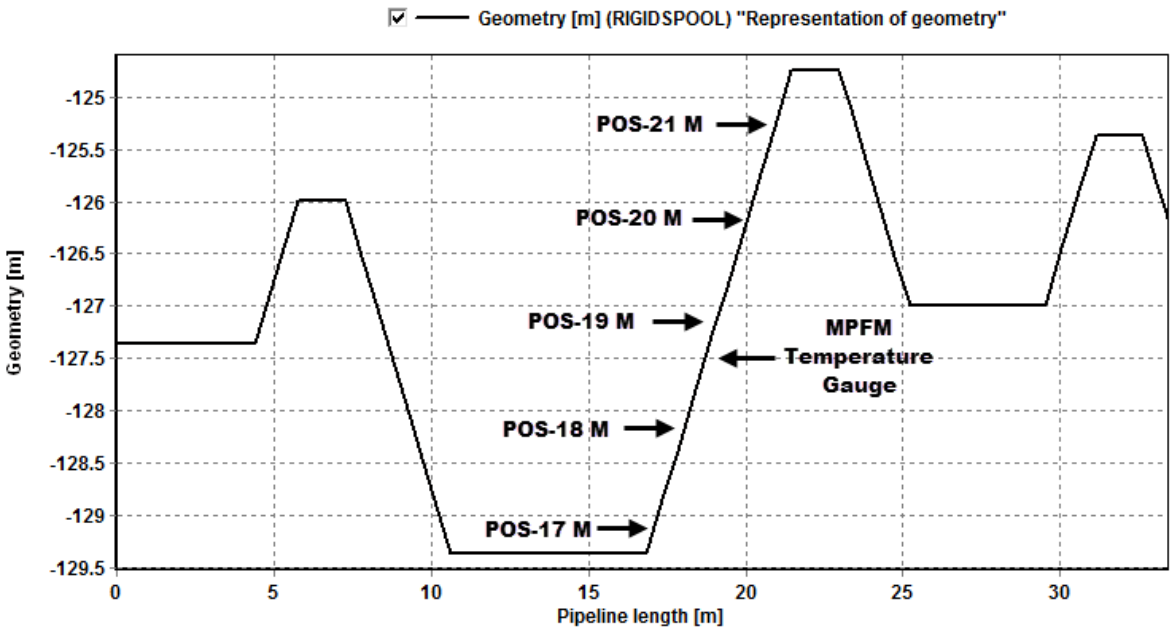

Figure 36: Location of temperature trends and MPFM temperature gauge

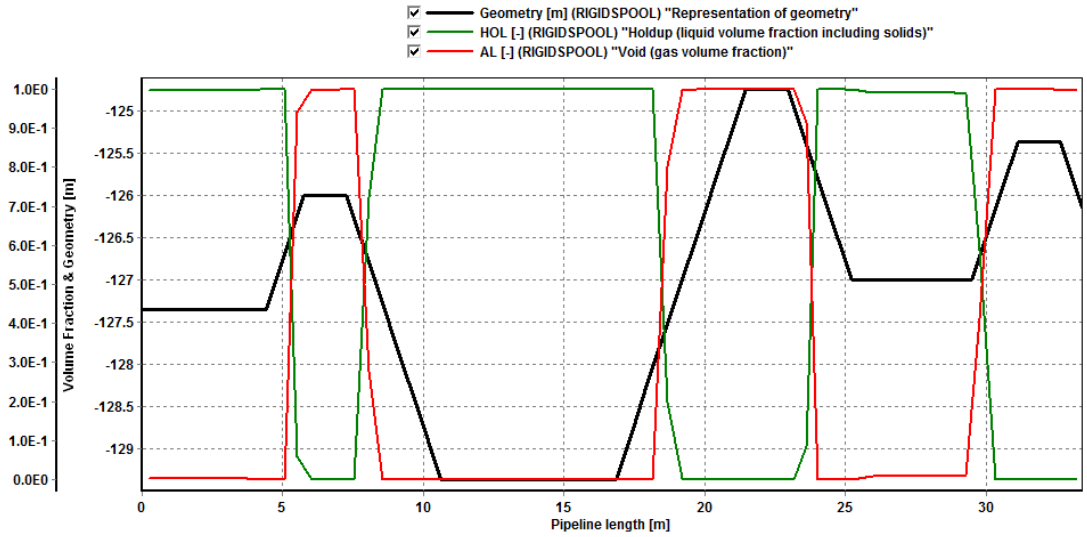

Figure 37: Rigid spool liquid and gas fractions after shut-in

The hydrate kinetics modeling within OLGA accounts for the exothermic reaction that occurs when hydrates form; it can be seen within the model this heat release starts around 25 hours near POS-18M (~16°C and 5,400 kPa). Based on the actual data from the MPFM position evidence of an exothermic reaction occurred close to 65 hours into the cool down period (~4°C and 5,400 kPa). It is important to note that the sub cooling is an input assumption within the hydrate kinetic model, which in this case the default suggested value of 3.6 °C.

Figure 38 illustrates the simulation prediction of total volume of hydrate throughout spool and expected mass.

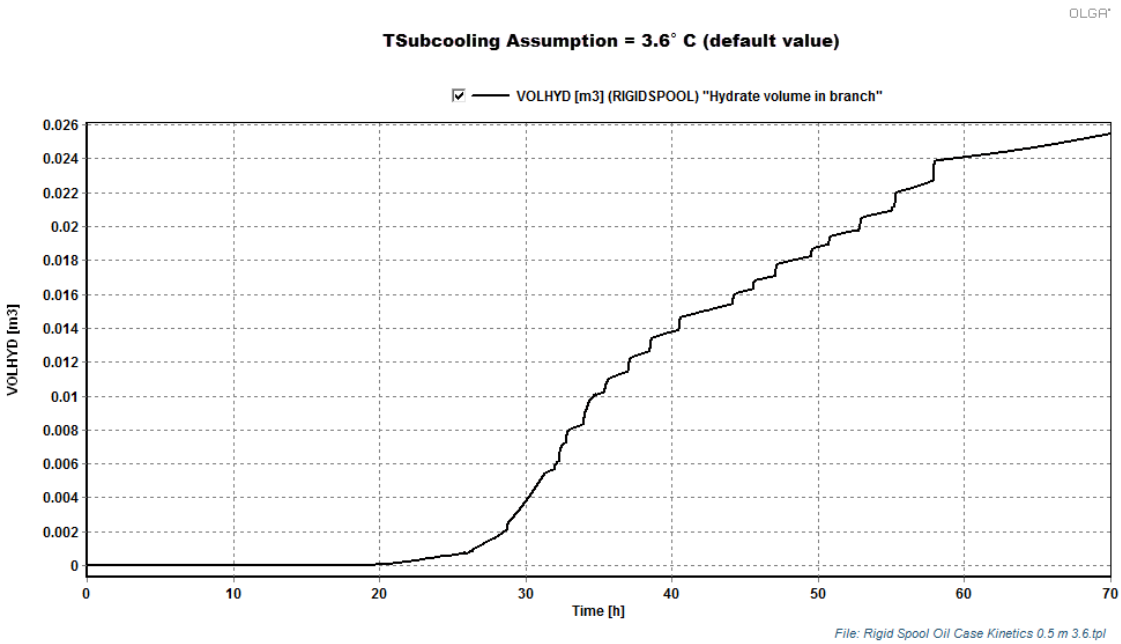

Figure 38: Model volume of hydrate over time within spool (Tsub = 3.6°C)

At approximately the 20 hour point some hydrate formation is started in the spool. There was a significant jump with regards to volume of hydrate predicted throughout the majority of the rigid production spool close to the 30 hour point. The hydrate mass prior to the 30 hour point is related to the pipe volumes that are predominately gas filled and cooled slightly quicker.

Figure 39 shows the predicted hydrate volume fraction (BEHYD) within sections of the rigid spool overlaid with the actual geometry of the spool.

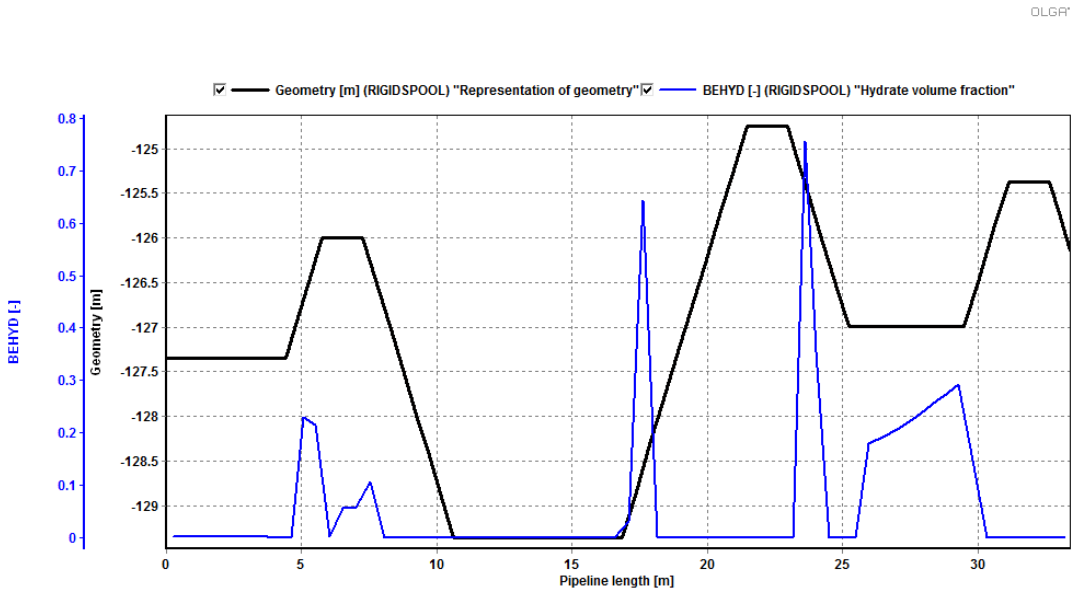

Figure 39: Hydrate volume fraction within spool

It is illustrated that there is likely hydrate throughout the spool with the highest portion just under 80% volume fraction within the area near and downstream of where the MPFM is located.

A sensitivity model was also considered by altering the default sub cooling temperature required to cause hydrate growth. Figure 40 shows the results of the sensitivity of sub cooling at 8°C versus the sub cooling assumption at 3.6°C.

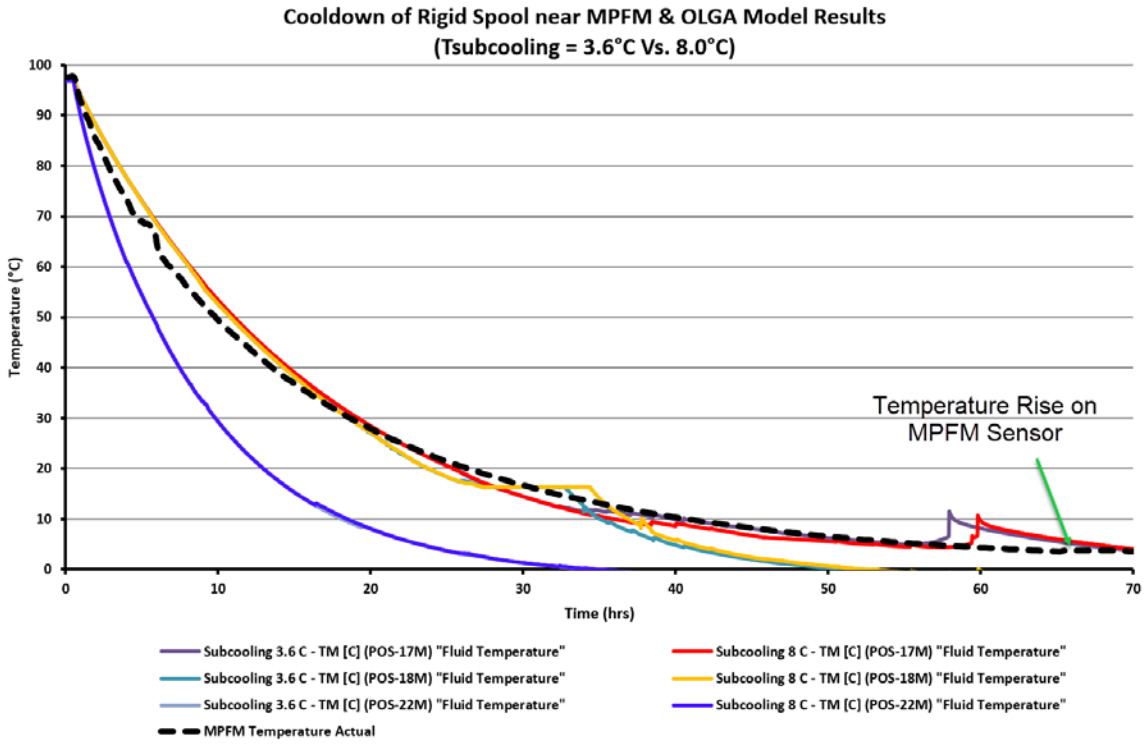

Figure 40: Subcooling sensitivity 8°C - cooldown of rigid spool near MPFM

At POS-18M it didn't make a big difference in timing but extended the time length which temperature was held. Figure 41 shows the time over which hydrate material is predicted to form between both scenarios, the initial hydrate formation is shown to be the same, but slightly after the 30 hour time there is a lag in hydrate growth for the 8°C subcooling case.

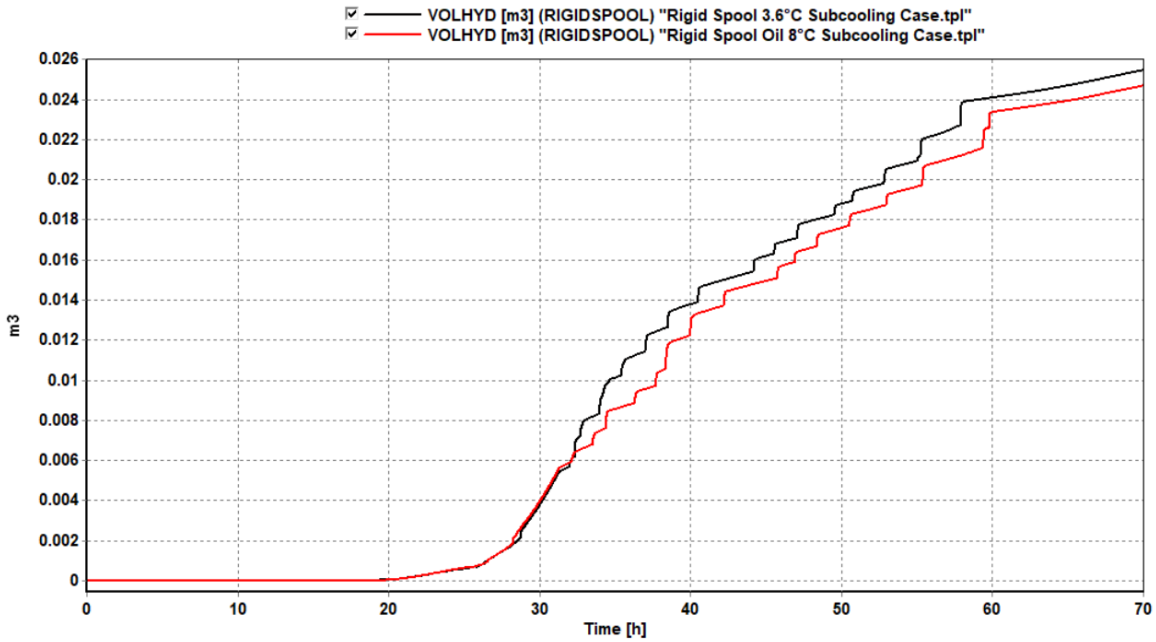

Figure 41: Hydrate volume formation sensitivity 8°C Vs 3.6°C subcooling

4.3 Discussion

Based on the comparison of the OLGA model and the real field data, the thermal cool down prediction was in good agreement with the location with predominately liquid phase and MPFM sensor. Having correct temperature transient prediction is important when considering the hydrate plug formation risk. The field data supports what the modeling is predicting for likely locations of highest hydrate volume since the blockage was located downstream of the MPFM. Within the field data, communication was shown between the tree and the MPFM located on the rigid production spool. It also shows that hydrate exists throughout the spool in smaller fractions.

There is evidence to suggest that the actual timing of the hydrate formation predicted by the model is slightly early. The assumption within the default kinetics model is that it takes 3.6°C sub cooling to initiate hydrate formation; this could prove to be possibly conservative in some cases. The initial exothermic reaction within the model occurred at POS-18M, close to the liquid/gas interface. For this particular position, the results of the sensitivity 8 °C Vs. the 3.6 °C sub cooling didn't make sense as the reaction occurred at the same time, when one would think it should be delayed. In the model the exothermic reaction occurred around 58 hours near the POS-17M, the MPFM sensor which a similar cooldown trend on temperature seen a temperature rise approximately at 65 hours. It should be cautioned that the spool was dead and with little disturbance during this period, which likely supported the delay of hydrate formation. A slight pressure change from the downstream of the dead leg seemed to initiate the hydrate reaction.

Overall it demonstrates that this sort of modeling can possibly be a useful tool to give more insight for visualization of the situation for risk assessment and operational planning related to this particular situation; a blockage is confirmed. The next chapter of this report examines a situation where hydrate formation were present with the same modeling tools.

5.0 Production Flowlines outside of NTT

5.1 Field Data - Production Flowlines outside of NTT

Within chapter 4.0 an example of a hydrate blockage was given where the subcooling time was met. This section will outline the field data of interest for which it was known that there were potential hydrate conditions within the production flowline infrastructure. The facility of interest was operating offshore when an emergency shutdown occurred and went outside of its suggested no touch time (NTT) of 6 hours due to topsides complications. The facility and flowline layout were previously discussed in chapter 3.4.2. Figure 42 once again summarizes with the subsea production systems and the location of drill centers.

Figure 43 illustrates the events that occurred at a high level showing a timeline of subsea pressures along with riser return temperature. Note that the pressure and temperature data is flat lined for a period which is related to what caused the ESD; the data is not real as the systems flat lined with no data available. The following points summarize the significant events corresponding to the numbers in Figure 43:

1. A plant trip had occurred approximately 12:40 AM

2. Flowlines were left stagnant until 11:40 AM for a total duration of 11 hours. During this duration subsea pressures (based on MPFM and tree sensors) fell from 4,800 kPa to 4,200 kPa due to the pressure settle out and flowlines cooling down. Blowdown of the flowlines commenced around 11:40 AM with subsea pressure falling to approximately 1,800 kPa.

3. At 4:20 PM preheating the lines by hot-oil circulation starts; the flowlines up to this point had been dead for 15.5 hours.

4. Hot-oiling the flowloop finishes at 7:30 PM.

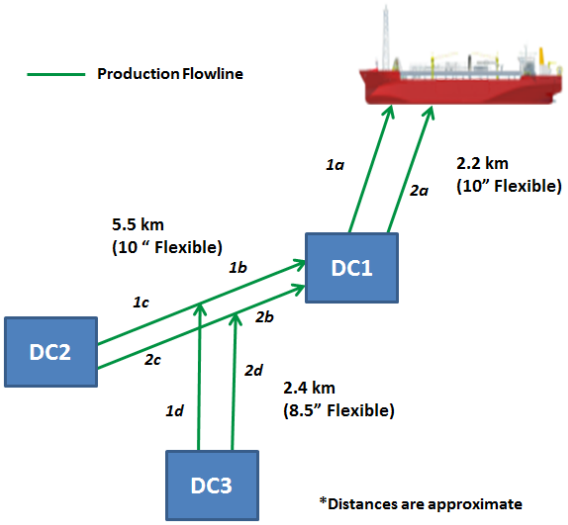

Figure 42: Overall production flowline layout

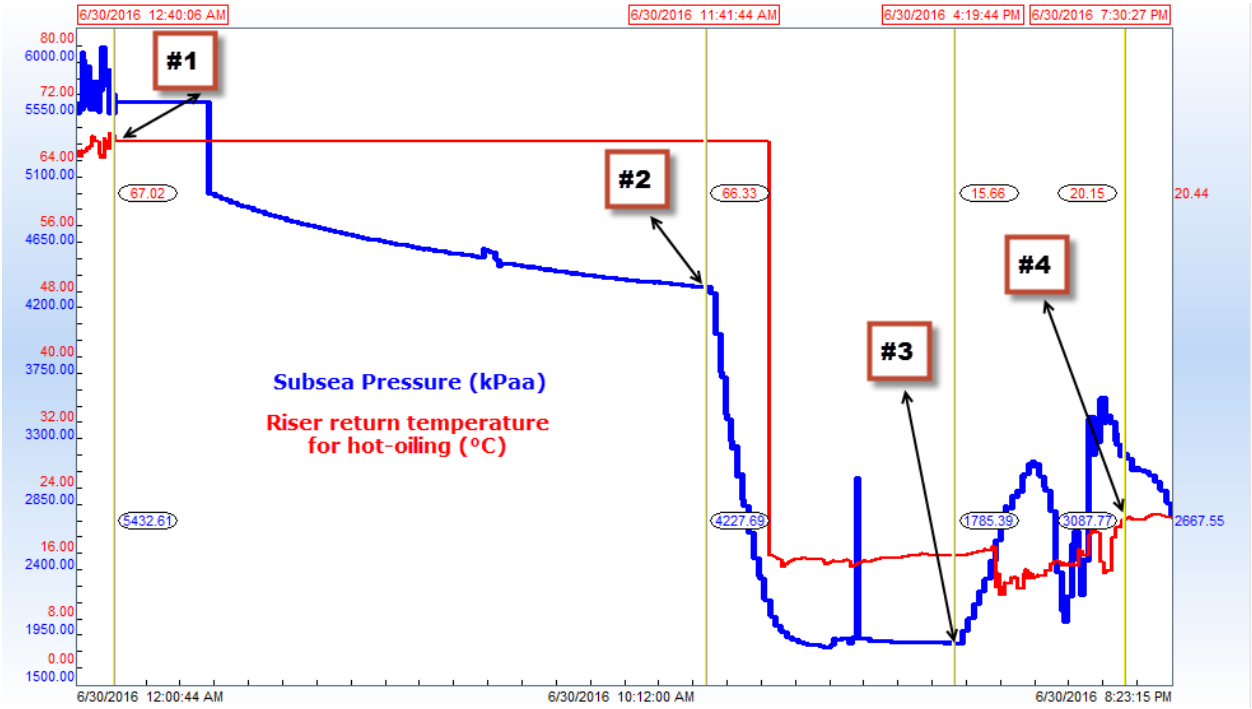

Figure 43: Field ESD timeline

Prior to the plant trip, temperature and flowrates of wells are measured through MPFMs. This data is important to modeling the conditions of the flowlines prior to the plant trip. Table 11 summarizes the input conditions to the mass nodes at each drill center/flowline within the OLGA model. The methodology behind compiling these conditions is using the MPFM measurements, a combination of calibrated gas lift choke calculation and venturi meter measurements for gas lift and considering the daily proration for the plant production volumes. Mass nodes that represent more than one well within the model use a weighted temperature average that is based on the total mass from the wells and corresponding temperature measurments.

Table 11: Summary of well rates & temperatures prior to ESD

Drill Center-Flowline	Oil (kg/s)	Water (kg/s)	Gas (kg/s)	Gas Lift (kg/s)	Temperature (°C)	Comment
DC1 - 1a	2.93	2.50	1.60	0.13	62	1 well
DC1 - 2a	9.78	20.66	3.10	3.52	79	2 wells
DC2	8.31	33.90	0.99	5.62	69	4 wells balanced in flowline 1c & 2c
DC3-1d	15.40	9.45	7.63	-	88	1 well, no gas lift
DC3-2d	9.05	1.39	5.85	-	74	1 well, no gas lift

5.2 Modeling

In order to model this situation a 3-step approach was taken within the OLGA simulator using the model files and restarts (restarts with conditions from previous models at the end point of the simulation model):

1. The first model was to establish the steady state flowing conditions of the flowlines and the long term shut-in. This modeled the conditions from Point #1 to Point #2 as outlined in Figure 43. Flow rates summarized within Table 11 were utilized along with setting the FPSO riser pressure nodes at 2,800 kPag.

2. The second model was used to blowdown the flowlines; from Point #2 to Point #3. In this case the riser pressures were brought down to 1,000 kPag.

3. The third model was used for hot oiling of the flowlines; from Point #4 to end of the hot oil circulation sequence. In this modelling step the field data around hot oiling circulation pump rate and temperature were input at a mass time series within the OLGA model. Note that the purpose of this model is to check for any hydrate risk during hot-oil and assess the temperature prediction performance of the model.

To evaluate the performance of the model, Table 12 and Figure 44 compare the field data to the model in terms of pressure and temperatures.

Table 12: Field data Vs Modeling

	Field data	OLGA model
Steady State Flowing - Riser #1 temperature (°C)	62	65
Steady State Flowing - Riser #2 temperature (°C)	66	66
Steady State Flowing - DC1a manifold pressure (kPaa)	4,600	4,600
Steady State Flowing - DC1b manifold pressure (kPaa)	5,300	5,100
Steady State Flowing - DC2a/b manifold pressure (kPaa)	5,600	5,514
Steady State Flowing - DC3a manifold pressure (kPaa)	6,400	6,100
Steady State Flowing - DC3b manifold pressure (kPaa)	5,800	5,600
Subsea settle out pressure prior to blowdown (kPaa)	4,300	4,300
Subsea pressure after blowdown (kPaa)	1,800	1,300

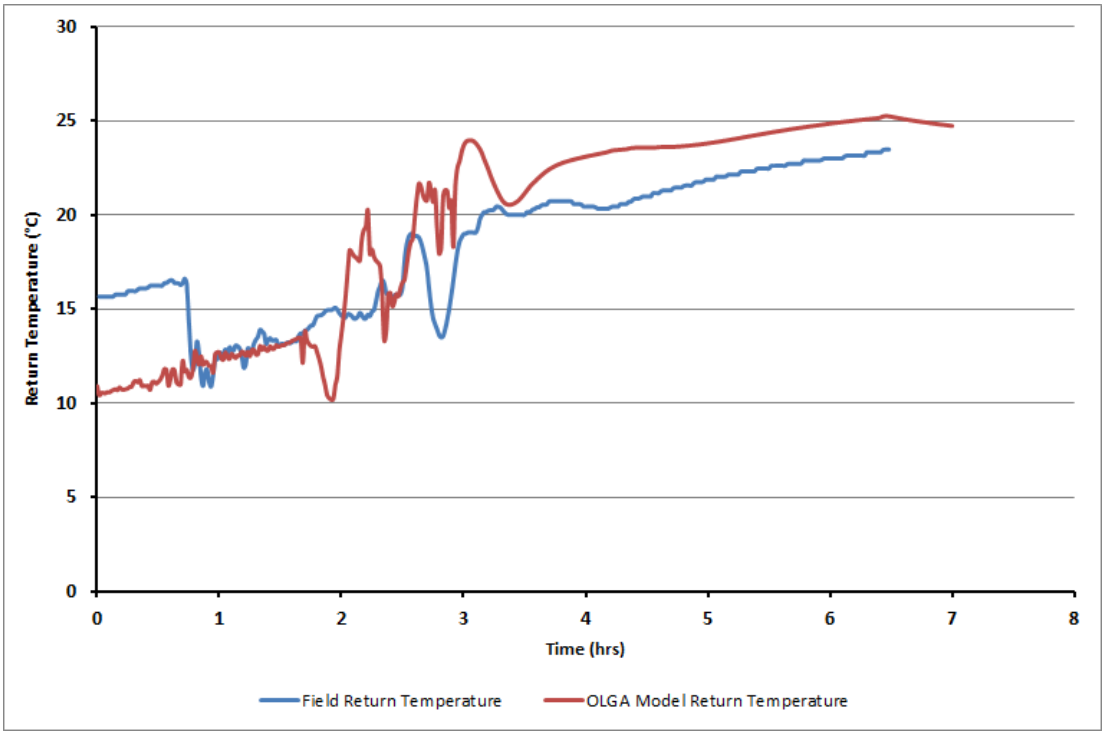

Figure 44: Riser return temperatures during Hot-oiling

It can be seen there is a good agreement between the model predictions and the data collected from the field. Note that within the field return temperatures during hot-oiling the temperature takes approximately 45 minutes to drop off at the sensor within topsides due to fluid starting to move, within the model the temperature is at the top of the riser, when the fluids are moving they are in good agreement.

The next set of results presented in this section illustrates what is of interest to this report of analyzing for hydrate formation and expected volume percent within flowline sections. Within all simulations the pipe/flowline segments with potential hydrate formation showed to be Segments 1a and 1b; from DC1 to the FPSO through the risers. In both cases results are similar so the analysis will focus on Segment 1a. All other flowlines did not show any hydrate risk due to the fact that the fluids were initially warmer and some flowlines had more insulation. Note that the flowlines were depressurized after 11 hours. After depressurization leading into the hot-oiling the models did not show any risk of hydrate formation. For the purpose of a sensitivity analysis, the model was extended to a 20-hour shut-in.

Figure 45 illustrates volume fractions of gas, oil and water within geometry from the DC1 drill center to FPSO during the shut-in period and after pressure settle-out.

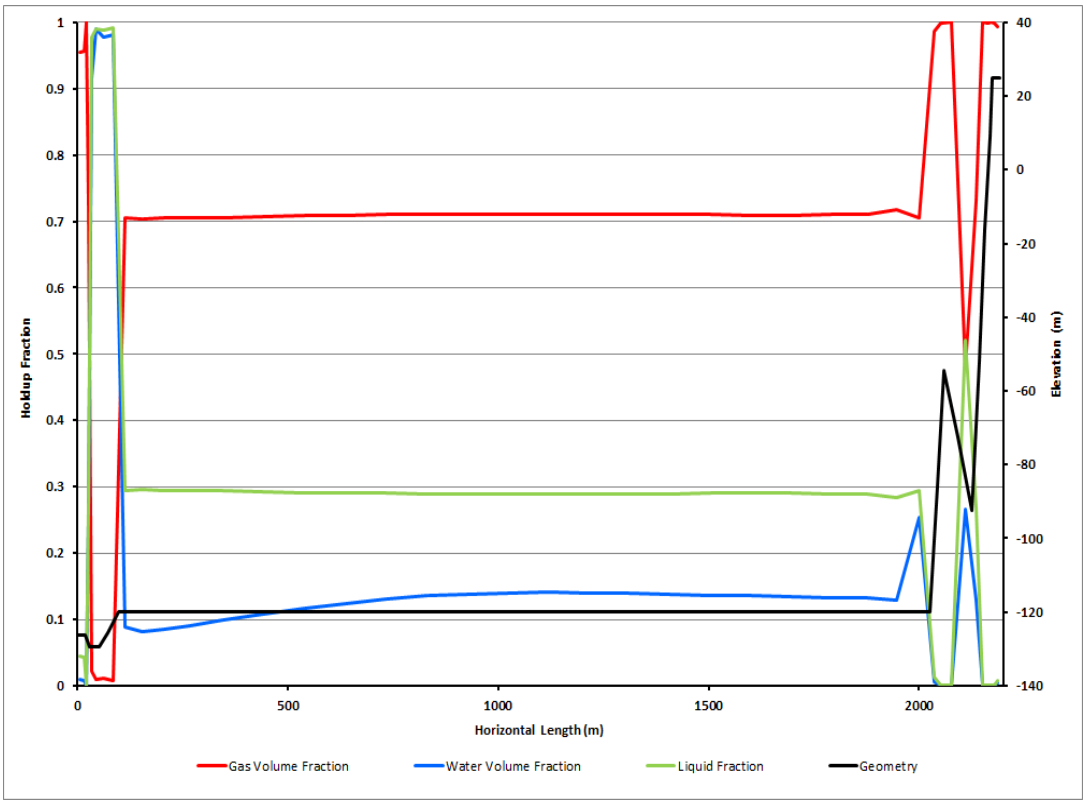

Figure 45: Shut-in Volume Fractions of Gas, Oil, and Water

The model shows some gas being left in the manifold of the drill center and predominately water within the flowline segment inside the excavated drill center. It also shows segments within the riser system where it is predominately gas.

Figure 46 illustrates DTHYD (how far temperature is from hydrate dissociation curve at a pressure) over time.

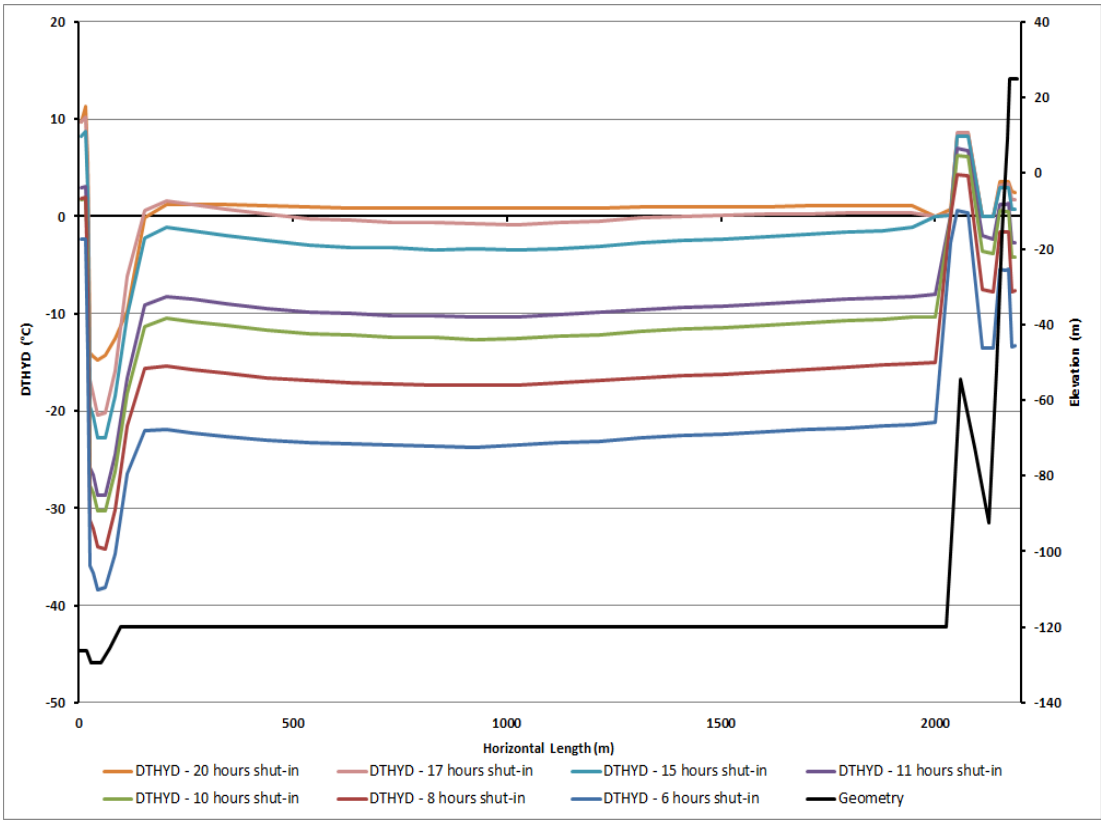

Figure 46: DTHYD-Segment 1a

Some segments filled predominately with gas start entering the hydrate zone approximately 6 hours after shut-in. Regions where DTHYD goes greater than 0°C are areas predominately filled with gas, thus it does not necessarily have hydrate risk as water is required for hydrate to form.

Figure 47 illustrates the predicted volume of hydrate formed within Segment 1a during the shut-in period.

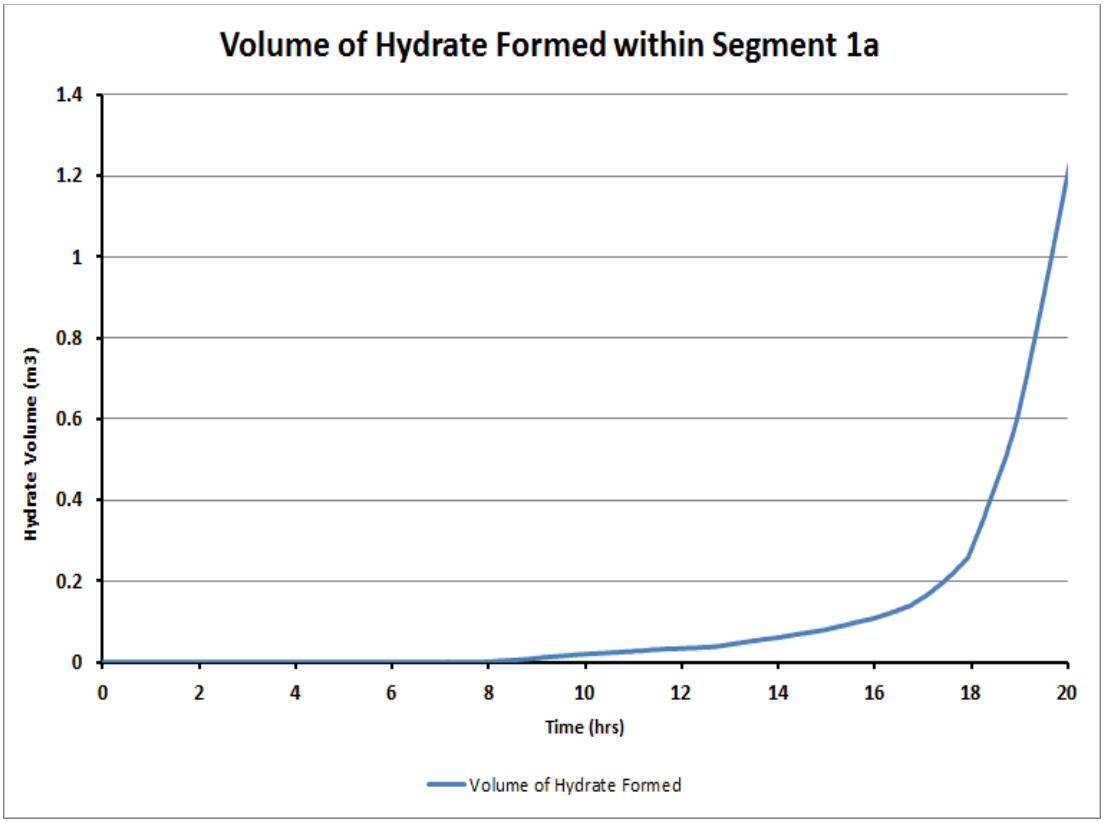

Figure 47: Volume of Hydrate Formed - Segment 1a

Some hydrate is predicted to start forming around 8 hours, but in negligible amount. At 11 hours into the shut-in time the total hydrate volume within the branch is <0.03 m^3, thus little risk of hydrate blockages. Around 17 hours it can be seen that the onset of hydrate starts accelerating rapidly; at 20 hours of shut-in it is predicted that greater than 1 m^3 of hydrate existed within the flowline segment.

Figure 48 illustrates predicted hydrate volume fraction (BEHYD) within Segment 1a geometry.

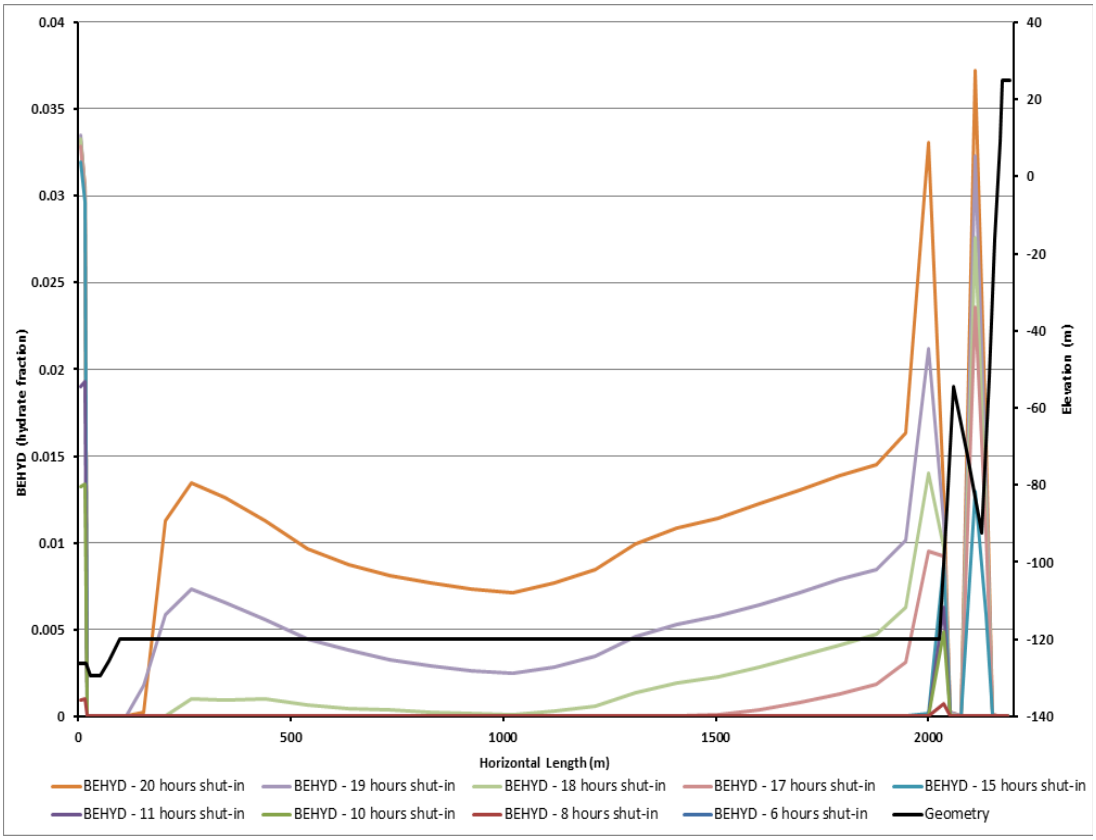

Figure 48: BEHYD (hydrate volume fraction) - Segment 1a

The first areas where small fractions of hydrate could be formed were at the drill center manifold and near the base of the riser. The hydrate continued to grow throughout the model simulation time; the volume fractions at these points around 11 hours were <2 % at the drill center manifold and < 1% at the base of the riser. It can also be seen that around 17 hours the potential hydrate started to grow more rapidly throughout the flowline segment.

5.3 Discussion

In this section of the report the real field data was extracted and attempts were made to relate them to multiphase thermohydraulic modeling to predict potential for hydrate formation. The model included a complex subsea system that connected several oil production wells to an FPSO. The modeling based on temperature and pressure comparisons were in a very good general agreement with reality, which supports temperature and pressures predictions inside the flowlines. This is important for predicting when hydrate conditions occur. The modeling included taking the subsea production system through steady state, shut-in, blowdown, and fluid circulation by hot-oiling.

By coupling the transient multiphase simulator with a hydrate kinetic model, a better understanding of hydrate blockages risk can be assessed. The model can provide the ability to predict temperatures, pressures, and fluid content within the flowlines. In this case it was shown even though the production system went beyond its accepted NTT by 5 hours there was very little chance for hydrates to form within the flowlines in substantial amount to form a plug. It would have likely been acceptable to restart production wells between 12-14 hours

after being shut-in. The flowlines would warm quickly from the wells starting to flow in this case. The little hydrate fraction based on the model that may have existed near the drill center manifold would have likely been taken care of by the warmer fluids from the well or warm water just sitting on the downstream. It is also important to note that the default subcooling input of 3.6°C was utilized in the modeling as well; this may be conservative based on work in previous section and the hydrate curves were based on lift gas with pure water (e.g. no salt).

In comparison to the hydrate work completed by Kinnari [10], the system would have been sitting inside the green area of their notional induction time, which would represent >12 hrs NTT.

There may be even more opportunity to push the operating envelope even further as literature info has suggested that hydrate volume fractions <20% generally does not present risk to actual plugging [25] [11]. For example, it would be interesting to see if any hydrate plugging could occur when opening a well 20 hours after shut-in. Of course, understanding the hydrate particles agglomeration and potential for more hydrate formation will be important to investigate in this case.

The hydrate equilibrium diagram utilized within the model was based on lift gas composition and water, which may be slightly conservative by a couple of degrees centigrade. The modelling could be improved if there was potential to produce hydrate curves based on every pipe segment volume within the model. This should be feasible with OLGA and the compositional tracking. Another improvement could be potentially building a way into the model to account for the sub cooling to better predict hydrate crystal formation as a function of fluid mixture, time, and degree of sub cooling.

The other interesting area to address would be that the model in its current state is based on oil-dominated system, results may differ with sections that may be water/gas dominated. This would be applicable to a shut-down start-up situation, since fluids will segregate and on start-up there could be potential for water dominated systems within pipe sections and as fields mature they are more likely to become water dominated. Finally, another parameter that could affect the results is the stability of emulsions of the oil-water mixture. It has been reported that the OLGA model tends to over predict the coalescence of oil and water; this would likely have an effect on hydrate formation and actual free water within the system [11].

Overall this example has shown how a simulation tool supported with field and experimental data can be used to analyze the situations where hydrate plugs could form. The modelling tool and the presented methodology can enable operators to make informed decisions and develop appropriate operating procedures to maximize production efficiency.

6.0 Conclusion and Recommendations

This work has demonstrated applicability and usefulness of a multiphase simulator and a hydrate kinetics prediction tool to real oil field operating problems. As offshore production infrastructure age and developments of such fields become economically challenging, having well thought methodologies and software tools can help engineers to justify extending operating envelopes and improve oil production economics. It is a complex problem to integrate the whole hydrate formation and blockage phenomena within a model as there are many interacting variables. Making small steps develop engineering approaches and modelling techniques can prove as a useful tool for engineers to assess situations cautiously. The current strength of the CSMHyK module coupled within the OLGA software package is making a more realistic prediction of hydrate formation in lieu of relying on hydrate curves only.

A real scenario was demonstrated based on field data. In this scenario where hydrocarbons and water were left within a 30 m pipe, the modelling approach resulted in successful outcome as it predicted correctly the approximant likely location of the blockage based on the hydrate volume fraction. The default sub cooling assumption may have been to small based on exothermic reaction evidence, but this is likely to vary based on situations because of the stochastic nature of hydrate formation. Overall the tool demonstrated its value in predicting likely locations of hydrate material that are not necessarily blockages, which is beneficial to understand during operational planning and troubleshooting.

Application to a complex field scenario including kilometers of production flowline undergoing an actual shut down and start up was also carried out in this study. In this case the system went beyond the fields “no touch time” based on hydrate risk and was still operated without problem. The methodologies used in this study helped to demonstrate what situation was likely to happen within the flowlines. It was confirmed that reasonable thermal/pressure prediction can be modeled which is important to any hydrate formation scenario. It was also demonstrated in this case that the “no touch time” could be extended to broaden the operating envelope and improve the operators’ flexibility in managing subsea production systems.

The following recommendations are made to further improve the hydrate kinetics model:

- Sharing of other actual instances of hydrate blockages or operating within hydrate regions to compare to the tool’s predictions to validate and build confidence within the tool.
- Including a way to generate hydrate curves within each pipe segment of the model based on fluid contents.
- Incorporating a way to predict the stochastic nature of hydrate formation based on composition, time, and degree of sub cooling.
- Further understanding of how oil/water emulsions may affect the hydrate formation and blockage risk.
- Further understanding of acceptable hydrate volume fraction under various conditions and how it relates to predictions of hydrate kinetic modelling tools such as OLGA CSMHyK.
- Conducting flow and stagnant lab tests under controlled environment to benchmark the predictions of the software under controlled experimental conditions.

7.0 Works Cited

[1] D. Sloan, C. Koh, A. Sum, A. Ballard, J. Creek, M. Eaton, J. Lachance, N. Mcmullen, T. Palermo, G. Shoup and L. Talley, Natural Gas Hydrates in Flow Assurance - 1.3 Four Rules of Thumb Arising from Crystal Structure. (pp. 2,3,4), Elsevier, 2011.

[2] E. Hammerschmidt, "Formation of Gas Hydrates in Natural Gsa Transmission Lines," *Industrial and Engineering Chemistry,* vol. 26, no. 8, pp. 851-855, 1934.

[3] K. Kinnari, X. Li and L. Robins, "3D Gamma Tomogrpahy Tool cutting edge technology for hydrate plug detection - Presentation (Statoil/Tracercro)," 3rd Trondheim Gas Technology Conderence, Trondhium, June 2014.

[4] "Why are Gas Hydrates Important?," Heriot Watt Institute of Petroleum Engineering, [Online]. Available: http://www.pet.hw.ac.uk/research/hydrate/hydrates_why.cfm. [Accessed 6 June 2018].

[5] KBC Advanced Technologies plc., "Calculating hydrate formation and dissaociation," in *Multiflash PVT Helpl (version 6.0)*.

[6] KBC Advanced Technologies plc., "Hydrate formation and inhibition models," in *Multiflash PVT Help (Version 6.0)*.

[7] J. Sjöblom, B. Øvrevoll, G. Jentoft, C. Lesaint, T. Palermo, A. Sinquin, P. Gateau, L. Barré, S. Subramanian, J. Boxall, S. Davies, L. Dieker, D. Greaves, J. Lachance, P. Rensing, K. Miller, D. Sloan and C. Koh, "Investigation of the Hydrate Plugging and Non-Plugging Properties of Oils," *Journal of Dispersion Science and Technology,* vol. 31, no. 8, pp. 1100-1119, July 2010.

[8] S. Davies, K. Hester, J. Lachance, C. Koh and D. Sloan, "Studies of hydrate nucleation with high pressure differential scanning calorimetry," *Chemical Engineering Science,* vol. 64, no. 2, pp. 370-375, January 2009.

[9] D. Turner, G. Mahadevan and J. Lachance, "Hydrate Stable Start-up and Restart of Oil and Gas Production Systems," in *The Twenty-fifth International Ocean and Polar Engineering Conference*, Kona, Hawaii, USA, 2015.

[10] K. Kinnari, J. Hundsied, X. Li and K. M. Askvik, "Hydrate Management in Practice," *Journal of Chemical & Engineering Data,* vol. 60, no. 2, pp. 439-446, 2015.

[11] S. S. D. A. E. Jefferson Louis Creek, "New Method for Managing Hydrates in Deepwater Tiebacks (OTC 22017)," in *Offshore Technology Conference*, Houston, Texas, USA, 2011.

[12] I. (. f. E. Technology), "The History of OLGA," [Online]. Available: https://www.ife.no/en/ife/ife_news/2012/departments/process_and_fluid_flow_tech/historienomolga. [Accessed 05 02 2018].

[13] K. Bendiksen, D. Maines, R. Moe and S. Nuland, "The Dynamic Two-Fluid Model OLGA: Theory and Application (SPE 19451)," *SPE Production Engineering,* pp. 171-180, May 1991.

[14] Schlumberger, "The OLGA Model - Modeling Basics," in *OLGA User Manual Version 2015.2*, Schlumberger, 2015.

[15] J. Creek, D. Estanga and S. Subramanian, "Project Design Hydrate Management by Application of Multiphase Flow Similation Tools with Hydrate Formation and Transport," in *7th International Conference on Gas Hydrates*, Edinburgh, Scotland, United Kingdom, 2011.

[16] G. Hatton and V. Kruka, "Hydrate Blockage Formation - Analysis of Werner Bolley Field Test Data," Deepstar CTR 5209-1, 2002.

[17] E. D. S. A. K. S. C. A. K. Luis E. Zerpa, "Overview of CSMHyK: A transient hydrate formation model," *Journal of Petroleum Science and Engineering,* Vols. Volumes 98-99, no. ISSN 0920-4105, pp. Pages 122-129, November 2012.

[18] S. Davies, J. Boxall, L. Dieker, A. Sum, C. Koh, D. Sloan, J. Creek and Z.-G. Xu, "Improved Predictions of Hydrate Plug Formation in Oil-Dominated Flowlines (OTC-19990)," in *Offshore Technology Conference*, Houston Texas, 2009.

[19] C. Nascimento, Interviewee, *RE: OLGA Hydrate Kinetics (Email communication).* [Interview]. 18 8 2016.

[20] H. E. R. L. LTD., "Well A-17, Sample 43-02, Reservoir Fluid Study," Calgary, Alberta, March 2000.

[21] K. A. T. plc., "Equations of state available in Multiflash," *Multiflash PVT Help (version 6.0).*

[22] C. Nascimento, "Fluid Modeling Using Multiflash 6.0 in OLGA 2015," Schlumberger, Calgary, AB, 2016.

[23] P. Labratories, "Gas Compositional Analysis (pf16-0437-003-2)," St. John's, NL, 2016.

[24] D. T. C. S. C. Limited, "Recombination and Hydrate Studies (Wells CP1 and SP2)," Edmonton, Alberta, 2009.

[25] A. Kurup, O. Hernandez, T. Idstein, C. Zamora, L. Greenly and J. Anderson, "Pushing Conventional Boundaries of Hydrate Management in a Dry Tree Facility (OTC 27780)," in *Offshore Technology Conference*, Houston, Texas, 2017.

[26] A. Sinquin, X. Bredzinsky and V. Beunat, "Kinetic of Hydrates Formation: Influence of Crude Oils," in *SPE Annual Technical Conference and Exhibition*, New Orleans, Louisiana, 2001.

[27] A. Sum, C. Koh and D. Sloan, "Developing a Comprehensive Understanding and Model of Hydrate in Multiphase Flow: From Laboratory Measurements to Field Applications," *Energy Fuels,* vol. 26, no. 7, pp. 4046-4052, 2012.

[28] A. H. Mohammadi, H. Ji, R. Burgass, A. B. Ali and B. Tohidi, "Gas Hydrates in Oil Systems," in *SPE Europec/EAGE Annual Conference and Exhibition*, Veinna, Austria, 2006.

[29] B. Barnes and A. Sum, "Advances in molecular simulations of clathrate hydrates," *Current Opinion in Chemical Engineering,* vol. 2, no. 2, pp. 184-190, 2013.

[30] J. Boxall, S. Davies, J. Nicholas, C. Koh and D. Sloan, "HYDRATE BLOCKAGE POTENTIAL IN AN OIL-DOMINATED SYSTEM STUDIED USING A FOUR INCH FLOW LOOP," in *Proceedings of the 6th International Conference on Gas Hydrates*, Vancouver, British Columbia, 2008.

[31] L. Zerpa, "A PRACTICAL MODEL TO PREDICT GAS HYDRATE FORMATION DISSOCIATION AND TRANSPORTABILITY IN OIL AND GAS FLOWLINES (Thesis)," Colorodo School of Mines, Golden, Colorado, 2013.

[32] M. Yousif, "The Kinetics of Hydrate Formation," in *SPE Annual Technical Conference and Exhibition*, New Orleans, Louisiana, 1994.

[33] S. Davies, J. Boxall, C. Koh, D. Sloan, P. Hemmingsen, K. Kinnari and Z.-G. Xu, "Predicting Hydrate Plug Formation in a Subsea Tieback," in *SPE Annual Technical Conference and Exhibition*, Denver, Colorado, 2008.

[34] P. Mogbolu and J. Madu, "Prediction of Onset of Gas Hydrate Formation in Offshore Operations," in *SPE Nigeria Annual International Conference and Exhibition*, August, Lagos, Nigeria, 2014.

[35] L. Zerpa, D. Sloan, C. Koh and A. Sum, "Hydrate Risk Assessment and Restart-Procedure Optimization of an Offshore Well Using a Transient Hydrate Prediction Model," *Oil and Gas Faclilites,* vol. 1, no. 05, pp. 49-56, 2012.

[36] S. Davies, K. Hester, J. Lachance, C. Koh and D. Sloan, "Studies of hydrate nucleationwith high pressure differential scanning calorimetry," *Chemical Engineering Science,* vol. 64, no. 2, pp. 370-375, 2009.